



UNIVERSITY OF INDONESIA

**ELIMINATING OBC RECEIVER GHOST USING DUAL SENSOR
SUMMATION : CASE STUDY ON SAHMURA FIELD**

THESIS

**GUSTRIYANSYAH
0906576473**

**MATHEMATICS AND NATURAL SCIENCES FACULTY
PHYSICS GRADUATE PROGRAM
RESERVOIR GEOPHYSICS SECTION
DEPOK
JULY 2011**



UNIVERSITY OF INDONESIA

**ELIMINATING OBC RECEIVER GHOST USING DUAL SENSOR
SUMMATION : CASE STUDY ON SAHMURA FIELD**

THESIS

In partial fulfillment of the requirements for the Degree Master of Science

**GUSTRIYANSYAH
0906576473**

**MATHEMATICS AND NATURAL SCIENCES FACULTY
PHYSICS GRADUATE PROGRAM
RESERVOIR GEOPHYSICS SECTION
DEPOK
JULY 2011**

STATEMENT OF ORIGINALITY

The work contained in this thesis has not been previously submitted for a degree at any other higher educational institution. To the best of my knowledge and belief, the thesis contains no material previously published or written by another person except where due references are made.

Name : Gustriyansyah Mishar

NPM : 0906576473

Signed :



Date : 24th June 2011






APPROVAL SHEET

This thesis is applied by :

Name : Gustriyansyah Mishar
NPM : 0906576473
Department : Physics
Section : Reservoir Geophysics
Title : Eliminating OBC Receiver Ghost using Dual Sensor
Summation : Case Study on Sahnura Field.

Has already defended with Board of Examiner and approved as partial fulfillment of the requirements for the degree Master of Science on Reservoir Geophysics Section, Master Degree Program, University of Indonesia.

BOARD OF EXAMINER

Head of Session	: Prof. Suprayitno M.	()
Supervisor	: Dr. rer. nat. Abdul Haris	()
Examiner I	: Prof. Suprayitno M.	()
Examiner II	: Dr. Carlos Tarazona	()
Examiner III	: Dr. Charlie Wu	()

Stated on : Jakarta
Date : 24th June 2011

ACKNOWLEDGEMENTS

There were more than a few moment this years when I was extremely close to abandon this effort. The reason that I persisted was purely because of the helps and support from a handful of people in my life – My parents, My relatives and also Dr. rer. nat. Abdul Haris as my campus supervisor . Jean Jacques Chameau for being very fantastic “senior” for junior likes me, even though he had no direct affiliation to do so other than “Senior” generous nature. I am so grateful for this support.

I also would like to thank BP Indonesia, especially Mr. Yayat Supriyatna for his support in this project, also Elnusa Geodata Processing, for allowing my work schedule to be flexible when needed, and whole part of this universe for always reminds me that life is so damn beautiful

Author
2011

ABSTRACT

Name : Gustriyansyah
Study Program : Physics
Title : Eliminating OBC Receiver Ghost using Dual Sensor
Summation : Case Study on Sahnura Field.

Ocean Bottom Cable (OBC) acquisition techniques were introduced to fulfill streamer limitation on facing shallow obstacles prohibiting usage of long streamer strings and navigation of seismic boats of significant size. OBC receivers being set at the sea floor are subject to strongly damaging receiver ghosts and peg-legs when water depths more than 10m. Fortunately, this kind of strong and very polluting multiples can be efficiently attenuated by dual sensor summation technique.

Practically, there are differences between the two responses, which must be balanced before combining both sensors. The most significant differences are coming from sensor coupling and a multitude of oblique water arrivals bouncing in the water layer. Standard methods to solve the coupling differences are based on matching operator calibration, but these methods have worked pathetically at least for the OBC projects of the last years in Indonesia. Results shows good improvement when sensor coupling is enhanced during the acquisition phase. By assuming that the responses have been calibrated to present similar aspect and generating wavelet, amplitude matching is the next issue that should be solved, because the two sensors do not record the same parameters. Standard methods as simple Automatic Gain Control (AGC) or as introduced by Fred Barr or Robert Soubaras to deal with this issue did not work perfectly on this data sets.

This thesis presents a small extension of the initial model introduced by Fred Barr, allowing to explicit the differences between the two sensors responses and a technique based on hodograph analysis to solve amplitude balancing issue, that worked satisfactorily for this data set.

Key Words : Dual Sensor Summation, Receiver Ghost, Hodograph

ABSTRAK

Nama : Gustriyansyah
Program Studi : Fisika
Judul : Penghilangan *OBC Receiver Ghost* Menggunakan Metode *Dual Sensor Summation* : Studi Kasus pada Lapangan Sahnura

Teknik Akuisisi *Ocean Bottom Cable* (OBC) diperkenalkan untuk memenuhi keterbatasan *streamer* untuk menghadapi daerah dangkal maupun larangan menggunakan bentangan *streamer* dengan panjang tertentu dan batasan kapal navigasi seismik dengan ukuran yang tertentu juga. *Receiver* OBC dibentang di dasar laut sangat rentan dengan gangguan dari *receiver ghost* dan juga *peg-legs* ketika kedalaman air laut mencapai 10 m. Tetapi jenis gangguan ini dapat dilemahkan dengan menggunakan teknik *dual summation*.

Sederhananya, ada perbedaan antara kedua respons yang harus disamakan sebelum menggabungkan kedua sensor, perbedaan yang paling utama berasal dari faktor *coupling* dari kedua sensor dan juga repetisi dari penjalaran gelombang yang terjadi diantara dasar laut dan muka laut. Metode yang biasa digunakan untuk menyelesaikan perbedaan ini mengkalibrasi kesamaan operator, tetapi metode ini tidak berjalan baik pada beberapa proyek OBC di Indonesia belakangan ini. Hasil yang lebih optimal didapatkan ketika sensor *coupling* sudah ditingkatkan pada fase akuisisi. Dengan menganggap respon masing-masing sensor telah dikalibrasi dan disamakan dengan menghasilkan wavelet, penyamaan amplitude adalah problem berikutnya yang harus diselesaikan, karena kedua sensor tidak merekam parameter yang. Metode yang biasa digunakan seperti *Automatic Gain Control* (AGC) atau seperti yang diperkenalkan oleh Fred Barr atau Robert Soubaras untuk menyelesaikan masalah ini tidak berjalan dengan baik pada data thesis ini.

Thesis ini memperlihatkan sedikit pengembangan dari model awal yang diperkenalkan Fred Barr, melihat perbedaan antara kedua sensor dan juga teknik berdasarkan analisa *hodograph* untuk menyelesaikan masalah penyamaan amplitude, yang bekerja cukup baik pada data thesis ini dengan menggunakan *window* dimana *ghost* dan sinyal tidak berinterferensi secara kuat.

Kata Kunci : *Sensor Summation, Receiver Ghost, Hodograph*

TABLE OF CONTENT

STATEMENT OF ORIGINALITY	i
APPROVAL SHEET	ii
ACKNOWLEDGEMENTS	iii
ABSTRACT	iv
ABSTRAK	v
TABLE OF CONTENT	vi
1. INTRODUCTION	1
1.1 Background	1
1.2 Problem Statement	2
1.3 Thesis Objectives	2
1.4 Location of Study Area	3
1.5 Data Set	3
1.6 Methodology	4
1.7 Writing Scheme	4
2. THEORETICAL BACKGROUND	6
2.1 Ghost Characteristics	6
2.2 Dual Sensor	9
2.3 Dual Sensor in OBC case	10
2.3.1 Standard Model	11
2.3.2 Extended Model	13
2.4 Dual Sensor Summation	14
2.4.1 Matching Operator	15
2.4.2 Matching Amplitude	16
2.4.3 Dual Sensor Summation	17
3. PROCESSING	18
3.1 Pre-Conditioning Process	18
3.2 Matching Operator Analysis	20
3.3 Amplitude Calibration using Hodogram Analysis	23
4. RESULT & DISCUSSION	27
5. CONCLUSION	37
REFERENCES	39

CHAPTER 1

INTRODUCTION

1.1 Background

Dual Sensor was introduced in acquisition in late 1940's, as a technology developed to address the receiver ghost and peg-legs issue inherent to Ocean Bottom Cable (OBC) with stationery detectors set directly at the water bottom (Barr, 1997) in significant water depths. OBC is necessary not only in transition zones, in hybrid marine and land environments, but also for exploration around developing marine field obstructed by production related platform, and anywhere offshore where obstacles or shallow spots prohibit using traditional towed streamer acquisition. Nowadays, Dual Sensor is also sometimes proposed in streamer surveys, to allow for deepening the streamer depth in noisy areas.

Because of OBC lay out, geophone and hydrophone, which are standard components of the dual sensor, are located directly at the ocean bottom, with a water column above the sensors, in which reverberations are free to travel and multiply, generating typical noise that theoretically can be removed with Dual Sensor summation (Shoshitaishvili,2006). This kind of noise, resulting in infinite duplications of the primary reflected upgoing signal is called receiver ghost, for the first strong reverberation, and peg-legs for the subsequent train of reverberations. Geophone and hydrophone respond to different physical parameters, respectively the particles velocity and the change of pressure.

Both are generated by the same seismic perturbations and as a consequence, geophone and hydrophone records should show strong similarities despite their difference in nature. However, because one of the parameter is of vector type while the second is scalar, the two sensors respond with the same polarity to a vertical event traveling in one direction and with opposite polarities when the event reverses its direction. More precisely, primary reflections which arrive upward are received with the same polarity by the two sensors while ghost and peg-legs constrained in the water column above the sensors arrive downward and are received with opposite polarities. Hence a deterministic elimination of the multiples immediately results from summation of the records of the two sensors.

Pressure and velocity are of course of different natures and some kind of calibration is needed before summation. This calibration is a key point in the process.

Data that have been analyzed for this project show low signal to noise ratio at raw stage, with strong variation of noise level and characteristics due to the variety of the water column depth. Other kinds of noise such as random, ground roll, strong linear events traveling in the water layer, etc are also found in this data set. In addition, a karstified limestone layer with strong reflection coefficient absorbed most of the energy of the signal, resulting in very poor coverage of the deeper objectives. From all the obstacles above, Dual Sensor summation was applied to recover that frequency part of signal lost to receiver ghost and peg-legs effects that so formidably obscure the seismic data in its imaging ability for structural and stratigraphical analysis in oil exploration.

1.2 Problem Statement

OBC acquisition techniques were developed for transition zones where water depth is usually greater than 10m (Ugbor,2007). In such depths, receivers set at the sea floor are subject to the damaging effects of the receiver ghosts and peg-legs. This kind of noise can be efficiently removed by dual sensor summation technique. We propose to present an in depth study of Sahnura Field, where several blocks were recently acquired with OBC techniques, in water depths ranging from 10m to 70m, fitting the description of transition or obstructed area or simply where OBC techniques were proposed to improve existing poor quality data recorded with standard streamer technique. On this area, the elimination of the strong receiver ghost and peg-legs from raw data proves the effectiveness of Dual Sensor summation.

1.3 Thesis Objective

The main objective of this thesis is to get interpretable seismic data, the acoustic impedance is low at the top and base of reservoir and the shallower karstified limestone with karst blocks of 200m width or less of the carbonate sequence creates strong lateral velocity variations above the reservoir. All the

possible reflections on these markers repeat after delays created in the water layer and interfere with each other primary and multiple. Dual Sensor summation is the only effective and powerful method to eliminate this ghosting phenomenon on such data set.

1.4 Location of Study Area

Research area is located in Eastern part of Indonesia, Papua province, in Bintuni bay. The Highlight box on the map below represents the study area, Sahnura Field. It is located on Bay environment, shallow water condition with water depth varying between 10 – 70 m.



Figure 1.1 Location Map for Study Area (Google Map,2011)

1.5 Data Set

Data analyzed in this thesis was acquired in 3D mode and produced by Dual Sensor Ocean Bottom Cable (OBC) in several blocks of Sahnura Field in Papua and was made available by and thanks to BP Indonesia. OBC method is the most common technique used in transition area. It was also used in one of the block, “V block” in 40m-70m water depths as an alternative to poor quality data previously acquired with conventional streamer. Most of the results presented here come from the “V” set, the size of which being approximately 170 CMP squared kilometers in surface, for 78 squared kilometers of full fold coverage.

1.6 Methodology

All analysis was performed at Elnusa processing centre with CGG Geocluster system, a full seismic processing package, providing all pre-processing and processing steps from reformatting to imaging, and all QC tools at every stage of the sequence. Supporting the main software, this thesis also uses Microsoft Office application for reporting.

This flowchart shows below, that input geophone and hydrophone data needed denoise processing. It was noticed that noise considerably affected the quality of sensor matching and the denoise pre-processing stage had actually to be very intensive to attenuate unwanted noise such as linear created by the source and propagating in the water layer, spiking, non-linear effects due to sensor coupling, etc.. Summation process was always QCed at each step. Matching operators were validated according to their reliability in terms of shape and uniformity from all attributes. Mean while, the top of the kartzified dominant event provided a solid interface with its ghost delayed by 50 to 100 ms, not interfering with responses of the bottom, for the Hodograph analysis. A reflection coefficient map was derived from the results of this analysis, applying relations (2.2) and (2.3), which was used to QC the computations.

1.7 Writing Scheme

This thesis consisted from several of chapter that will discussed about how to eliminate receiver ghost using dual sensor summation. In the first chapter, will discuss about ghost behavior first, to get same level of knowledge about what kind of noise that being faced for this thesis, after that dual sensor technique, especially on Ocean Bottom Cable (OBC) acquisition. It also discussed about standard model, that being introduced by Fred Barr, and a little improvement that done with this thesis and also the theory of Dual Sensor Summation. Second Chapter will discuss about how it works, from pre-conditioning process, matching operator analysis, and amplitude calibration using hodogram analysis. Last chapter will showing the results of methods that being done on this thesis, and it will be wrapped up with discussion about the effectiveness of this method.

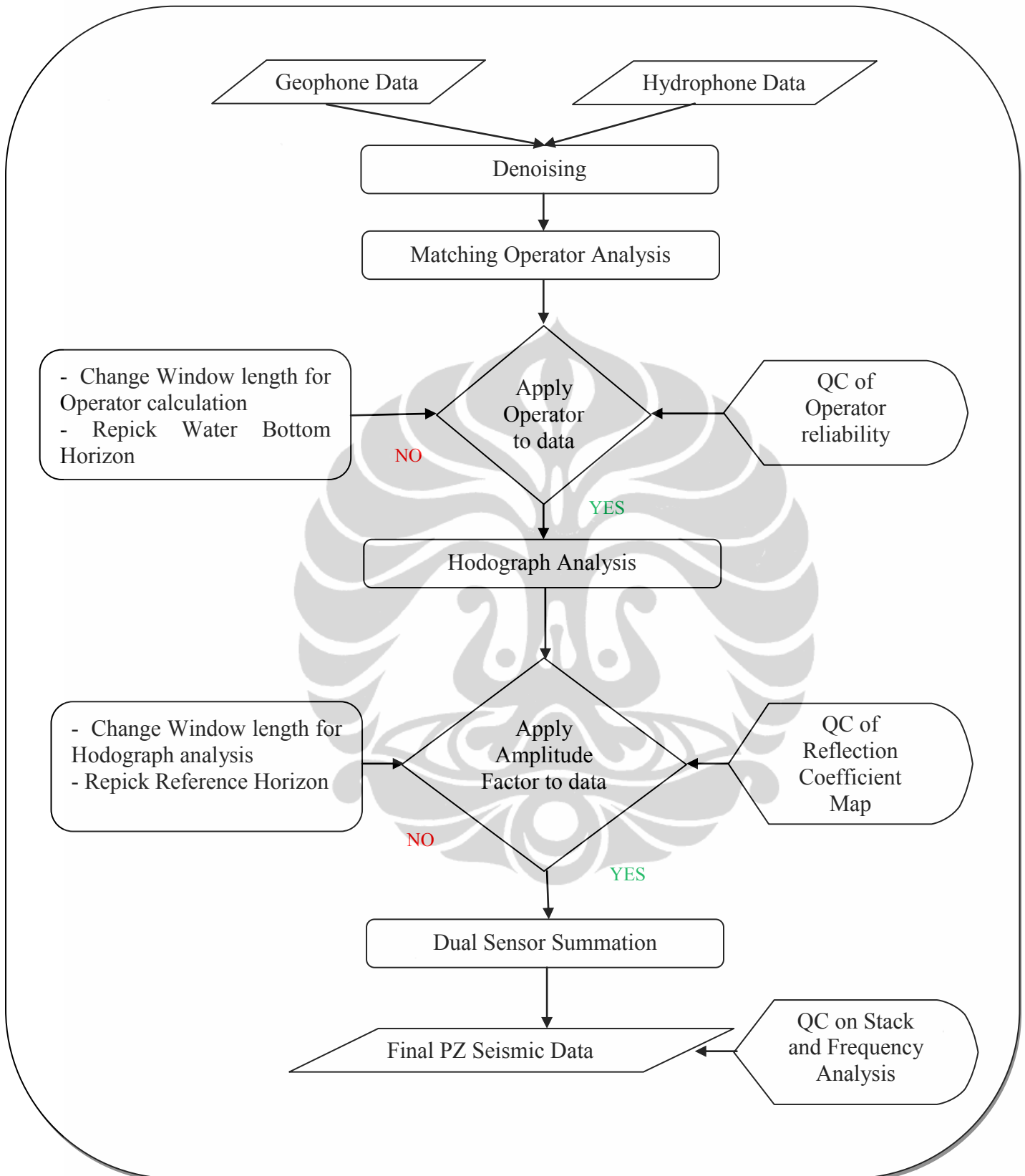


Figure 1.2 Flow Chart of Dual Sensor Summation Process

CHAPTER 2

THEORETICAL BACKGROUND

Dual Sensor summation is aimed to cancel the receiver ghost and peg-legs train which are recorded on top of the ground primary reflectivity response, of which they are multiples, by combining the responses of two sensors mounted on OBC cables, located at the sea floor. We will start by describing the reverberations which are created in the water layer above the sensors.

2.1 Ghost Characteristics

A receiver located at the sea floor not only records the ground reflectivity response, or « primary event » -P- as an upcoming wave, but also the reflection of this primary after it has bounced back at the sea surface to return downward and be recorded again as a duplication of the primary, called « receiver ghost » -G- .

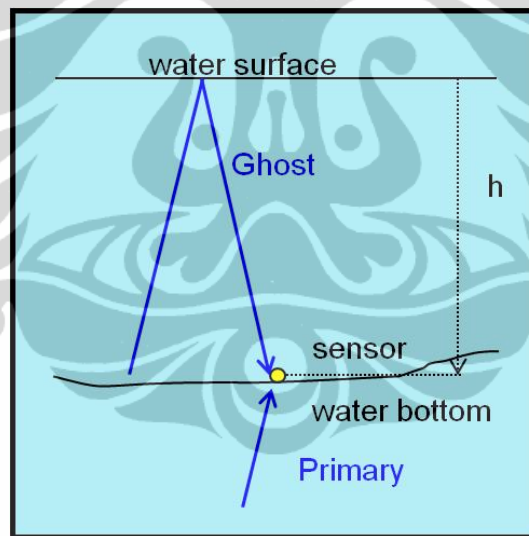


Figure 2.1. Ghost Phenomenon recorded by OBC Sensor in Space Domain

This phenomenon is a typical pollution that is inherent to OBC techniques, when ghost and primary are collided on seismic data, resulting in the destruction of frequency components, right in the useful seismic band. For instance, frequency components at 0, 25, 50Hz,etc. would cancel out by superimposition of the two events, from the response of a hydrophone below 30m of water, while frequency components at 12.5, 37.5Hz,etc. would be strengthened, giving the data a low frequency aspect with general low signal to noise (S-N) ratio. The ghost

operator is defined by the reflection coefficient at the sea surface, which is -1, the direction propagation which has turned from upgoing to downgoing after the reflection and the delay due to the two-way travel in the water layer.

The reflection coefficient of -1 at the free surface means no loss of energy for the ghost which, unfortunately, will bounce as strong as the primary. The change of propagation direction is the factor on which the Dual Sensor summation procedure is built for ghost cancellation as it will be described later on. Finally, the most important parameter driving the ghost aspect is the water depth. When water depth is lower than say 7.5m, the ghost is close enough to the primary (less than 10ms) to join it in the constitution of the wavelet while the first frequency notch is at 100Hz for a hydrophone. Water depths greater than 10m, become a serious problem of multiples needing to be solved.

As the receiver ghost is created by the primary, receiver peg-legs are created by the receiver ghost which, when reaching downward the water floor, is reflected back upward to create another reverberation in the water layer. This first peg-leg is to the ghost what the ghost is to the primary except that its strength is reduced by a factor linked to the reflection coefficient at the sea floor (with values from less than 0.1 to 0.3 or little more). Of course, each peg-leg in turn, generates another peg-leg in the same way.

Theoretically, the best subsurface image requires every reflective interface be represented by a single, short-duration wavelet on each trace. The reality of wave propagation consists of signal infinitely bouncing in the water layer above the bottom-cable's sensors, completely reflected downward at the water surface and partially reflected upward at the water bottom. Each reverberation in the water layer generates first the receiver ghost and then a peg-leg train until the energy vanishes.

Because of their reduced energy, the peg-legs can be addressed by deconvolution procedures, although these procedures would bring noise. In very Shallow water (Water depth < 10m), deconvolution also does a credible job of collapsing the receiver ghost into the original wavelet. For water depth greater than 10 m, the time gap separating the original wavelet from the receiver ghost becomes too long to be addressed with deconvolution algorithms. This problem

being ignored, each reflective horizon would be represented with several wavelets interfering with other reflections, perplexing the geological meaning on it.

The receiver ghost effect also shows up strongly in frequency domain and in “phase domain” as illustrated hereafter respectively on a real streamer’s hydrophone case and on a synthetic single reflection. In frequency domain, the ghost phenomenon creates a series of true notches (Soubaras, 1996), as demonstrated by the following sequence:

$$\begin{aligned}
 \text{Ghost delay:} & \quad \Delta t = \frac{2 \cdot d}{c} \\
 \text{Ghost operator for a hydrophone, in time domain:} & \quad \delta - \delta_{\Delta t} \\
 \text{Ghost operator for a hydrophone, at frequency } f: & \quad 1 - e^{i \cdot 2\pi \cdot f \cdot \Delta t} \\
 \text{Frequency notches (zeros of previous relation):} & \quad f_n = n \cdot \frac{c}{2 \cdot d} \quad (2.1)
 \end{aligned}$$

where, f_n = notch frequency (Hz), c = acoustic velocity of water (m/s), d = water depth (m), δ is the Dirac unit impulse, $\delta_{\Delta t}$ is the Dirac unit impulse delayed by Δt , and n is a positive integer.

For instance, in water depth of 11m, the first spectral notch will occur at 68.18 Hz, the water velocity being 1500 m/s, as shown on figure 3 below.

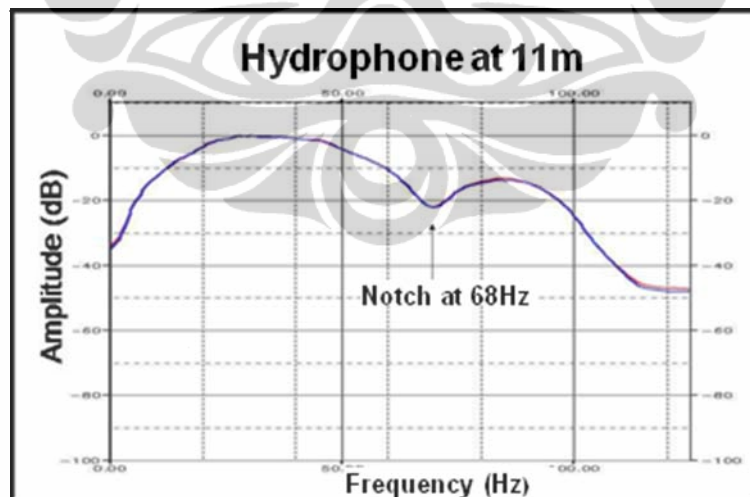


Figure 2.2 Ghost Phenomenon on Frequency Domain

The following synthetic example illustrates the ghost phenomenon from a “phase” point of view, considering a single zero phase initial wavelet and the receiver ghost in different water depths:

- Significant water depth, $\Delta t = 60$ ms, primary and ghost are well separated and do not interfere on each other. The wavelets are in phase on a hydrophone record and on a vertical geophone record, while their ghosts are of opposite polarities.

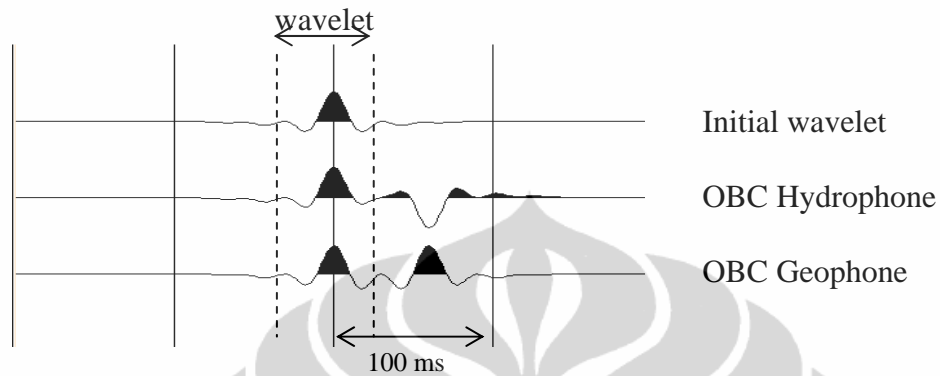
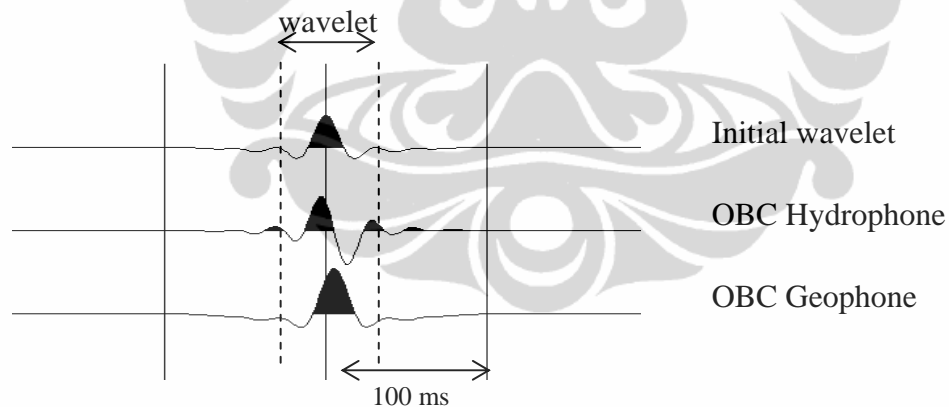


Figure 2.3. Ghost phenomenon in "Phase Domain" with $\Delta t = 60$ ms

- Shallow depth $\Delta t = 10$ ms, the primary and its ghost produce a unique wavelet, different of the original one, the geophone record being in phase with the initial wavelet while the hydrophone phase looked shifted bFigure



2.4. Ghost phenomenon in "Phase Domain" with $\Delta t = 10$ ms

The differences of the responses of the OBC vertical geophone and of the OBC hydrophone will be described in further paragraphs.

2.2 Dual Sensor

Dual Sensor is used to eliminate receiver ghost and peg-legs, because it provides a simple quasi automatic way to separate ghost and peg legs from

primary using the combined characteristics of a vector sensor, geophone, with a scalar sensor, hydrophone. The method is based on the change of the propagation direction between the upgoing primary and the downgoing ghost and peg-legs, yielding polarity differences between the responses of the two sensors. The polarity of a compressional wave is given by the direction of propagation:

- the particle velocity, measured by a geophone, is positive when the particle velocity is directed with the propagation,
- the change of pressure, measured by a hydrophone is positive when it is created by an action in the direction of propagation.

Then for an upgoing field (P), a positive event is directed upward and creates a positive change of pressure on the hydrophone while the particle velocity is projected positively onto a vertically oriented geophone. After reflection at the surface, where the coefficient is -1 , the particle motion reverts on its support and opposes the propagation direction which has become a downgoing field (G). The resulting change of pressure is then negative on the hydrophone while the velocity still directed upward remains projected positively onto the vertical geophone. By this simple way, Geophone and Hydrophone summation can add together the primary events while cancelling out the receiver ghost and all the receiver peg-legs. This is shown in figures 6 below:

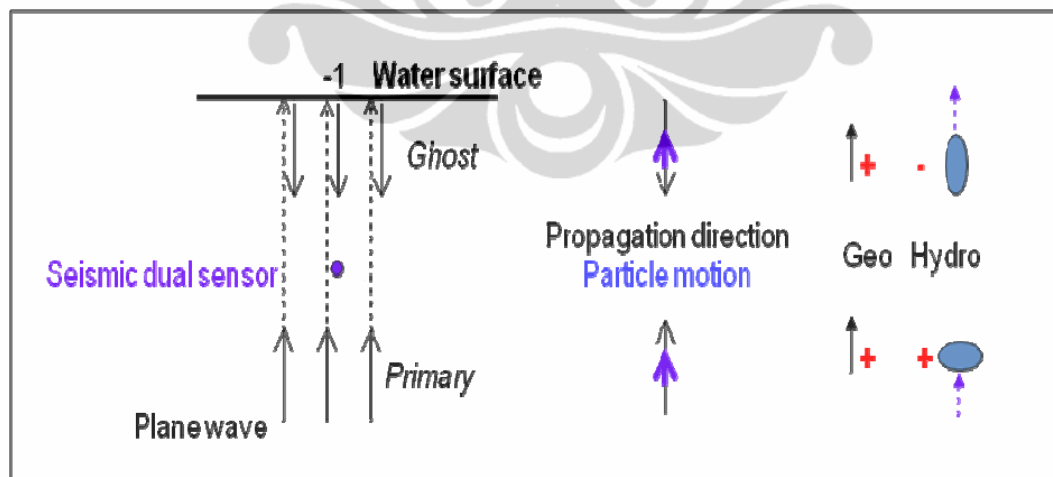


Figure 2.5. Geophone & Hydrophone Characteristics as Dual Sensor

2.3 Dual Sensor in OBC Case

In the OBC case, the following assumptions are made:

- The sea floor is locally flat and horizontal
- The primary event is vertical and so are the receiver ghost and peg-legs according to the first assumption
- The waves are plane-waves in pressure mode (P-waves) and there is no conversion according to the previous assumptions.
- The Dual Sensor is located at the sea floor.

The last assumption requires some attention. Being at an interface, the sensors do not record a pure incoming wave, as the primary for instance, but all the waves in the same side of the interface, whatever being the side according to continuity conditions in elastic mode. When the primary P reaches the interface, it is transmitted upward as P_t in the water layer but part of it, P_r , is reflected down and the sensor records the transmitted element P_t which equals the sum $P + P_r$. This introduces the reflection and transmission coefficients of the sea floor interface and shows that the receiver ghost is an image of P_t rather than of P . When the sensor receives the ghost, for the same reason, it also records its reflection on the sea floor and this happens for all peg-legs.

It is well known that at an interface, even at vertical incidence, the one-way reflection coefficients are not identical in pressure and in term of particle velocity. This yields discrepancies between the hydrophone and the geophone responses which might add some difficulties in the Dual Sensor summation theory as previously described. The situation was explicit by Fred Barr who modeled the reverberations in the water layer.

2.3.1 Standard Model

Each ray of the reverberations is affected the signed amplitude coefficient due to the presence of the interface: the upcoming primary P is transmitted as $P_t = t_u \cdot P$, t_u being the upward transmission coefficient, then bounces back at the surface to become $-P_t$, the downgoing ghost.

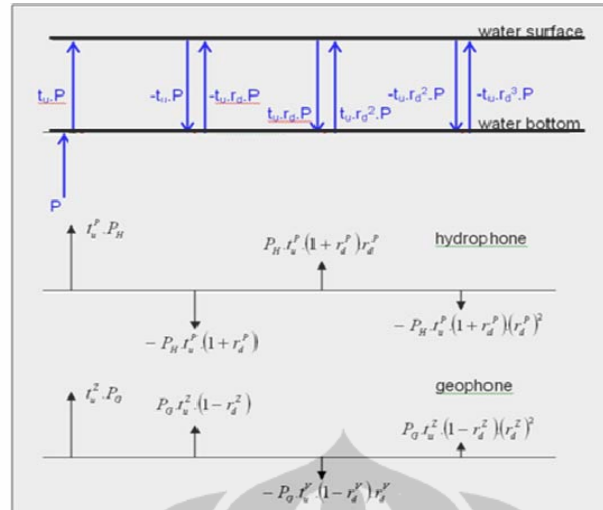


Figure 2.6. Time domain Impulse Response of Barr Model with assumptions : P-mode, vertical incidence, plane-waves. (Barr,1997)

The next reflection at the sea floor results in $-t_u.r_d.P$ to generate the first peg-leg, where r_d is the downward reflection coefficient of the sea floor, and so on. All the rays are represented on top of figure 7 with horizontal shifts to avoid drawing confusion although they are on the same vertical. The lower part of the figure shows the scalar acoustic pressure response and the vector particle velocity response after projection on a fixed vertical axis, as time-domain impulse response of vertically propagating P-wave, and the delays between consecutive impulses represent the two-way travel time from water surface to water bottom. Note that the water surface reflection coefficient value is -1 in pressure mode as well as for particle velocity.

The first impulse at time $t=0$, is positive and normalized to unit amplitude for both parameters. The most important fact is that, as expected, pressure and vertical particle velocity are of opposite polarities for all the other events, ghost and peg-legs. Between the primary upgoing event and the downgoing multiples, the pressure changes its polarity once, at the sea surface, because of the negative coefficient, meanwhile the polarity of the vertical particle velocity is subject to two changes, first at the sea surface like the pressure, then after the change of propagation direction from upward to downward. The second fact is that, when the amplitudes of the primaries are equalized, the amplitudes of the ghost and peg-legs do not exactly correspond for pressure and particle velocity. However, the

ratio between the two parameters is the same for the ghost and each of the peg-legs and a calibrating factor depending on the downward reflection coefficient of the sea floor, can be applied first to one of the parameters to match the level of the multiples of the other parameter, before summation.

2.3.2 Extended Model

The previous model is not absolutely complete and should include the reflection of the primary, D_0 at the sea bottom and the transmission rays that are created each time the ghost or a peg-leg ($D_1, \dots, D_n \dots$) hits downward the water floor. Of course, those events, all downward, do not enter or exit the water layer but they will create in turn new responses of the ground which will re-appear as scaled copies of P .

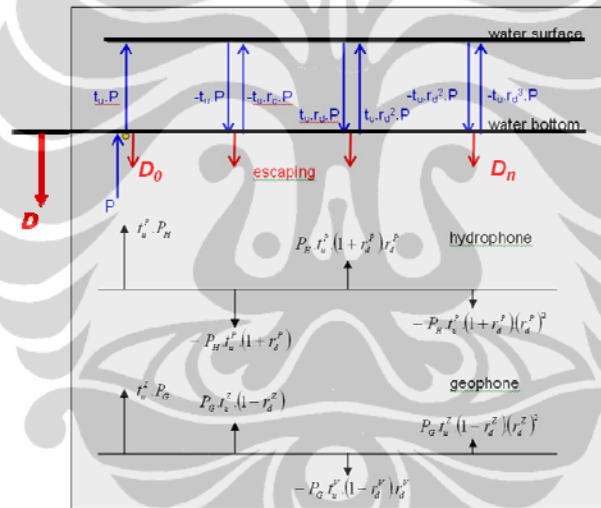


Figure 2.7. Time domain Impulse Response of Extended Model with assumptions : P-mode, vertical incidence, plane-waves. (modified from Barr,1997)

The responses presented in Barr’s model are due to a primary event itself created in response to an initial downgoing excitation D including the source term and all its reverberations. D is considered just below the sea floor, initiating and inputting into the model and yields $P=R*D$, R being the reflectivity response of the ground, including the internal multiples, excluding entry and reverberations in the water layer.

The primary itself, the ghost and every peg-legs re-issue energy into the model, escaping down from the water layer, each energy D_n generating in turn the

same kind of response $P_n = R^*D_n$ as shown in Figure 8. Of course, although being significant in each contact of the reverberations with the water bottom, each D_n is of reduced amplitude in front of D . These new sources should nevertheless be considered since there is only one “reflection coefficient” between D_1 and D , in the same ratio order as between the first peg-leg and the ghost.

This extended model results in the following harmonic responses recorded by the hydrophone (P) and the geophone (Z) when all waves are considered:

$$\begin{aligned} Z &= c_Z \cdot k_Z \cdot \left(\underbrace{1 - r^u}_{\text{(Primary)}} + \underbrace{t^u \cdot t^d \cdot e^{i\omega \left[\frac{-2h}{V} \right]}}_{\text{(Ghost)}} + \underbrace{t^u \cdot t^d \cdot \sum_{n \geq 2} [-r^d]^{n-1} \cdot e^{i\omega \left[-n \cdot \frac{2h}{V} \right]}}_{\text{(Peg-legs)}} \right) \cdot \frac{P(h)}{U} \\ P &= c_P \cdot k_P \cdot \left(\underbrace{1 + r^u}_{\text{(Primary)}} - \underbrace{t^u \cdot t^d \cdot e^{i\omega \left[\frac{2h}{V} \right]}}_{\text{(Ghost)}} - \underbrace{t^u \cdot t^d \cdot \sum_{n \geq 2} [-r^d]^{n-1} \cdot e^{i\omega \left[-n \cdot \frac{2h}{V} \right]}}_{\text{(Peg-legs)}} \right) \cdot \frac{P(h)}{U} \end{aligned} \quad (2.2)$$

where ω is the current angular frequency, c_Z and c_P are the instrument and coupling responses respectively of the geophone and of the hydrophone, k_Z and k_P the corresponding sensor types scaling, $P(h)$ the primary upgoing event expressed as a potential and measured at $z=h$, V the propagation velocity in the water layer and r^u , t^u , r^d , t^d the reflection and transmission coefficients upward and downward on the water floor, expressed in terms of potential. In addition, with R^0 representing the amplitude term of the ground reflectivity response:

$$U = 1 - r^u \cdot R^0 + t^u \cdot t^d \cdot R^0 \cdot e^{i\omega \left[\frac{-2h}{V} \right]} \cdot \sum_{n \geq 1} [-r^d]^{n-1} \cdot e^{i\omega \left[-(n-1) \cdot \frac{2h}{V} \right]} \quad (2.3)$$

Note that $U=1$ in the initial Barr's model.

2.4 Dual Sensor Summation

There are three steps to conduct this Dual Sensor summation methods, which are :

1. Computation of Matching Operators to equalize the wavelet shapes of the responses of the 2 types of sensors (geophone and hydrophone). Main differences stand in the coupling of the sensors, the scaling units and their instrument responses.

2. Estimation of Amplitude Factors to compensate for the different behavior of the velocity field and of the pressure field at the interface (different one-way transmission coefficients).
3. Dual Sensor Sum of calibrated hydrophone and geophone records

2.4.1 Matching Operator

The wavelet calibration can be done in several ways, depending on the selected working window:

- On a non interfered down-going event, at quasi vertical incidence (Ex direct arrival from quasi zero offset shot), separated from its ghost,
- On a dominant up-going event, at quasi vertical incidence, provided the ghost is delayed enough and there are no significant interferences
- On a window on the quasi vertical incidence reflectivity field, including reverberations and interferences, primaries and ghosts.

To validate this choice, Robert Soubaras introduced the cross-ghosting operation. Equations (2.2) can be further developed to produce:

$$\begin{aligned}
 Z &= c_z \cdot k_z \cdot \frac{C}{1 - R^0 \cdot B} \left[1 + e^{-i \cdot \omega \cdot \left[\frac{2h}{V} \right]} \right] \cdot P(h) \\
 P &= c_p \cdot k_p \cdot \frac{q \cdot C}{1 - R^0 \cdot B} \left[1 - e^{-i \cdot \omega \cdot \left[\frac{2h}{V} \right]} \right] \cdot P(h)
 \end{aligned}
 \tag{2.4}$$

Where

$$B = -e^{i \cdot \omega \cdot \left[\frac{2h}{V} \right]} \cdot \frac{\sigma}{\bar{\sigma}}, \quad C = +e^{i \cdot \omega \cdot \left[\frac{2h}{V} \right]} \cdot \frac{2}{\bar{\sigma}}$$

$$\sigma = (1 - q) + (1 + q)e^{-i \cdot \omega \cdot \left[\frac{2h}{V} \right]}$$

$$q = \frac{\rho \cdot V}{\rho_B \cdot V_B}$$

Where q being the water layer to subsequent layer impedance ratio.

In (2.3), the terms in brackets are exactly the expressions of ghost operators which would be free from the interface: the two spikes of each operator are of amplitudes +1,+1 for the geophone and +1,-1 for the hydrophone. They do not depend on the reflection coefficient at the sea floor and can thus be immediately

deterministically built. The cross-ghosted geophone response is obtained by convolving Z with the hydrophone deterministic ghost and the cross-ghosted hydrophone response by convolving P with the geophone deterministic ghost. By matching the two cross-ghosted signals, the searched match between the initial records is produced. A drawback of this is that the spectra of the two cross-ghosted signals include and mix the notches of both sensors and the matching operator must be chosen very short.

2.4.2 Matching Amplitude

After the matching operator is computed, its amplitude needs to be calibrated with a factor that depends on the downward reflection coefficient r^d at the sea floor.

This coefficient is usually unknown and methods focus on optimizing the geophone with hydrophone sum in a given sense: once an un-scaled matching operator o' is computed, the calibrated one $o = k \cdot o'$ can be estimated after scan for the varying coefficient k to provide the best sum $k \cdot o' * G + H$, for instance in terms of frequency content, where the ghost effect is expected to be damaging.

When a strong reflector shows up with its ghost, both dominant in front of possible interferences, the following method can be used:

- Consider the calibrated geophone $o' * G$ and the hydrophone H as the two components of a 2D vector
- Project or rotate this vector onto a direction where the ghost effect is absent.

This direction is found on the hodograms built from the two components.

The reflectivity field includes:

- P : Primary reflections with internal multiples, for which the calibrated geophone and the hydrophone are proportional
- R : Ghost and peg-legs (reverberations) for which the calibrated geophone and the hydrophone are proportional with a negative factor.
- N : Random noise

Hodograms for the particle motion represented by the 2 vector components extend and fold around a straight line through the 2 opposite quadrants of same polarity for the 2 components, where the P energy is not strongly interfered and around another straight line extending through the 2 remaining quadrants, where the R energy is dominant, shown in figure 2.8.

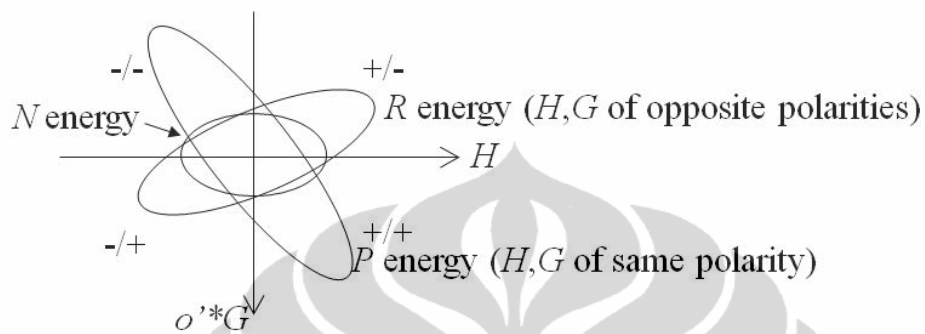


Figure 2.8. Hodogram Analysis

The advantage of this method is that it may address non linear cases, it is not dependent on strong short duration noise like spikes and it may be used in a very short time window (4-5 samples are sufficient). Longer time windows can also be envisaged, providing stacking effect. In addition, a map of the reflection coefficients at the water bottom can be produced from the found amplitudes.

2.4.3 Dual Sensor Summation

Once the matching operator is calibrated in amplitude for a receiver point, it can be applied to each single geophone trace of the receiver gather and Dual Sensor sum yields the “primary”, including internal multiples below the water layer but excluding the water layer receiver ghost and reverberations train.

The matching operator is purely a receiver attribute which can be computed on a stack of traces taken from a receiver gather, while the calibrating scalar, depending on the water bottom reflection coefficient, may also depend on the source to receiver offset, more precisely on the incidence of the upcoming reflection on the water floor. It is assumed constant over a receiver gather, valid for the reflections of interest.

CHAPTER 3 PROCESSING

3.1 Pre-Conditioning Process

As mentioned on the previous chapter, P and Z datasets that being used on this thesis is very low and signal to noise ratio even in the raw data, contaminated with noise and/or imperfect receiver coupling (Ball,2004). There are several pre-conditioning process that being done on this data set and :

- Swell Noise Attenuation

For towed streamer surveys, swell noise is caused by data acquisition in rough sea conditions, particularly when the cables are being towed at relatively shallow depth. Although originally designed and named for the type of noises generated by swells, the process works and is appropriate for any noise condition of limited extent in the domain being analyzed. The noise will be attenuated with resamples the data along the direction of the noise and measure the noise velocity.

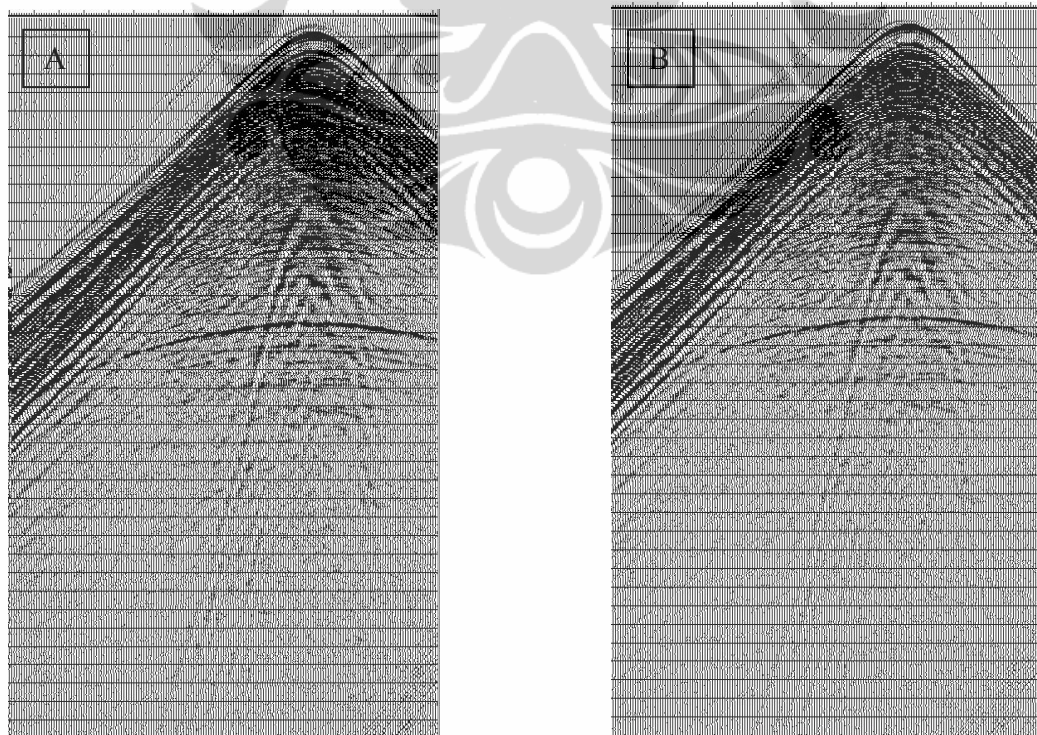


Figure 3.1 Comparison between (a). Common Receiver Gather before Swell Noise Attenuation applied. (b). Common Receiver Gather after Swell Noise Attenuation applied

- Velocity Filtering

Dipping noise that appear on raw gather data can be attenuated using 3D FK Filtering. In this domain, dipping events plot along straight lines (in-line and x-line) radiating outwards from the point of zero frequency and zero wavenumber (in the 3D sense, it appears as a cone). Gently dipping events plot closer to the frequency (vertical) axis (horizontal events actually plot along this axis), while steeply dipping events plot closer to the wavenumber (horizontal) axis. Events with a positive dip (that is, where the reflection time increases as the trace position increases) have positive wavenumbers and events with negative dips have negative wavenumbers. The events are therefore more easily separated in the f-kx-ky domain and unwanted events such as linear noise can be rejected by applying a user-specified filter. Velocity filter that being applied on this step are [5,10,2000,2500] m/s.

(Note: The term dip refers only to the apparent dip of an event measured in velocity (m/s) and not to the actual spatial dip of the geologic structure.)

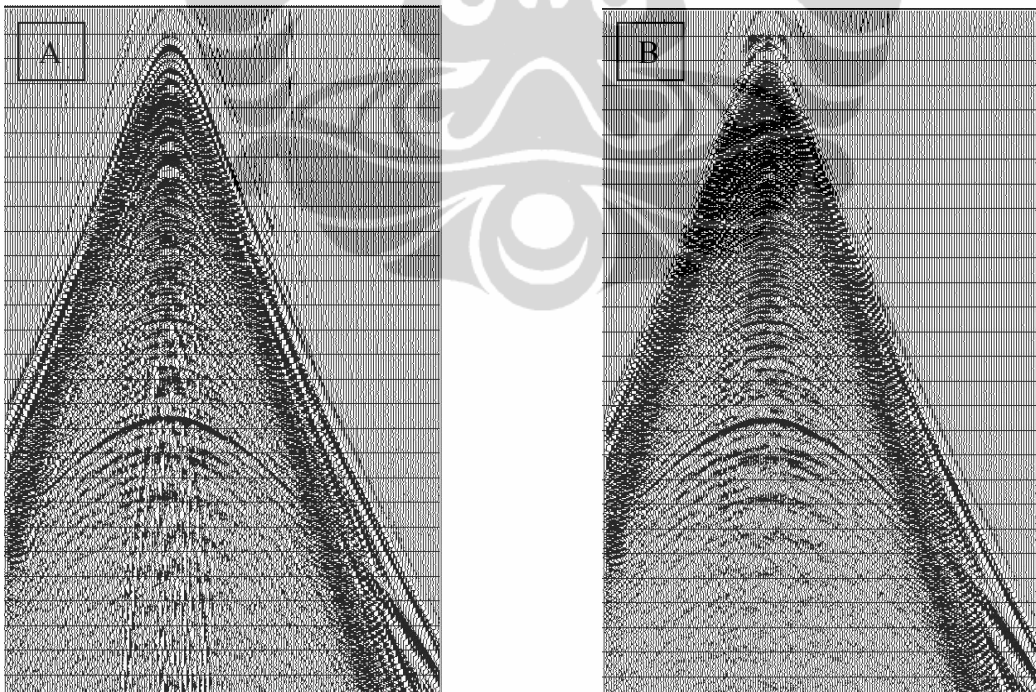


Figure 3.2 Comparison between (a). Common Shot Gather before Velocity Filtering applied.
(b). Common Shot Gather after Velocity Filtering applied

- Tau-p Deconvolution

This processing step is one of the most powerful to attenuated the reverberation train, but a remaining strong ghost still could not be attenuated without summation, This step is transforming data from t-x domain into Tau-p-q domain based on the vector offset in an areal gather. Operator length that being used in this process is 240 ms, and gap 40 ms after several test.

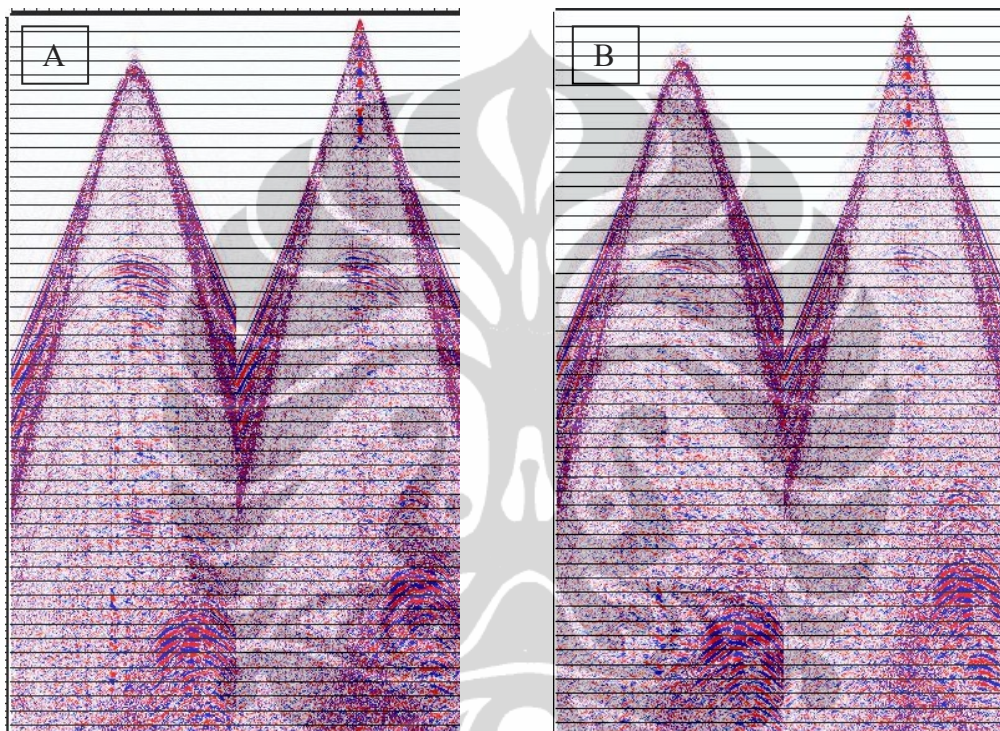


Figure 3.3 Comparison between (a). Common Shot Gather before Tau-Phi Deconvolution applied. (b). Common Shot Gather after Tau-Phi Deconvolution applied

- Discrete Wavelet Transform Decomposition

The wavelet transform was used as a 1D tool to decompose one trace in time domain into several versions with different frequency contents, all keeping visual seismic characteristics. This is actually the way a standard analysis works. Although the transform is 1D, panels were built in receiver gathers, per source line, which were assumed the optimum gathers for the given parallel geometry. No noise reduction method was applied on the panels, the noisiest ones only being removed, while great care was taken to fully preserve the initially weak signal.

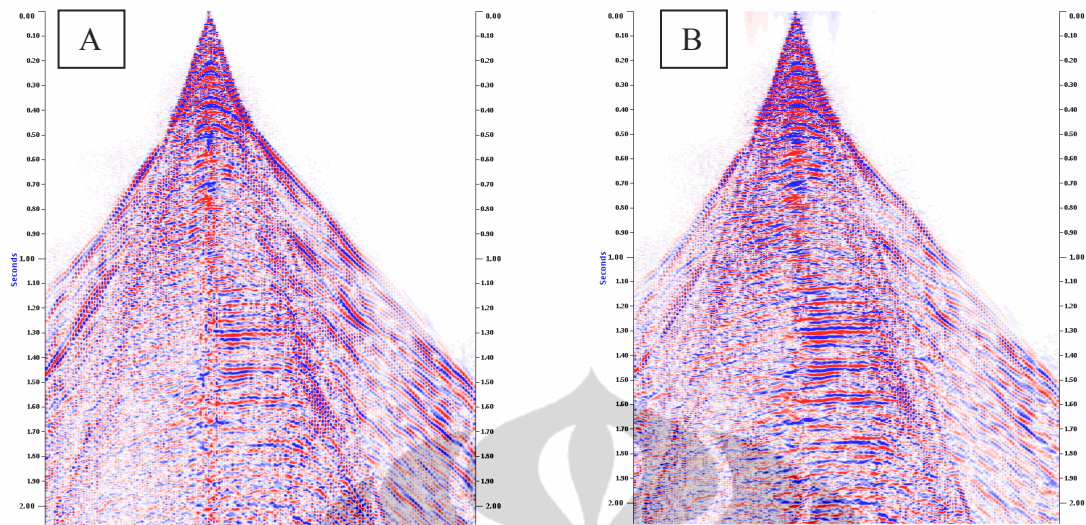


Figure 3.4 Comparison between (a). Common Receiver Gather before Discrete Wavelet Transform Decomposition applied. (b). Common Receiver Gather after Discrete Wavelet Transform Decomposition applied

3.2 Matching Operator Analysis

The Derivation of matching operator analysis can be performed after a wavelet with convenient signal to noise ratio is available in both hydrophone and geophone datasets after de-noising process done. Wavelet that being used in this thesis was tested to calculate on selected working windows, a non interfered down-going event, at quasi vertical incidence (ex. Direct Arrival or First Break).. (Specht,2007).In data set that being used in thesis, the first break could not be used for all receivers from the production data because there are some point that not having near offset. Fortunately, there are extra special records called PO lines (“P” positioning, and “O” Orientation done in 2D mode with the source passing above the receivers, delivering direct arrivals, this PO lines avoid problems that appeared on first break that taken from near offset data from receiver line, which the first arrival is still overlaying between refraction and direct arrival from water layer.

1. First Break

From the first break, reverberations were also seen on both geophone and hydrophone data.

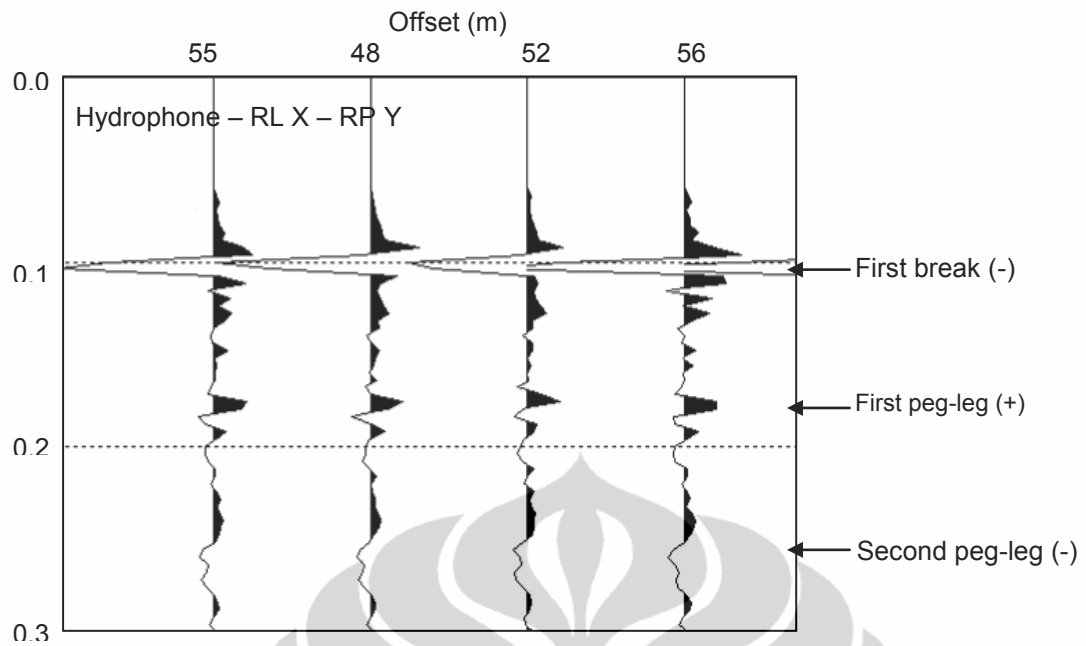


Figure 3.5 Evidence of reverberations on Hydrophone Data
(60m water depth)

On Figure above, the maximum of the flattened first break (down-going event) on the hydrophone data is represented by negative polarity, continued by first peg-leg is positive, and the second reversing again to negative.

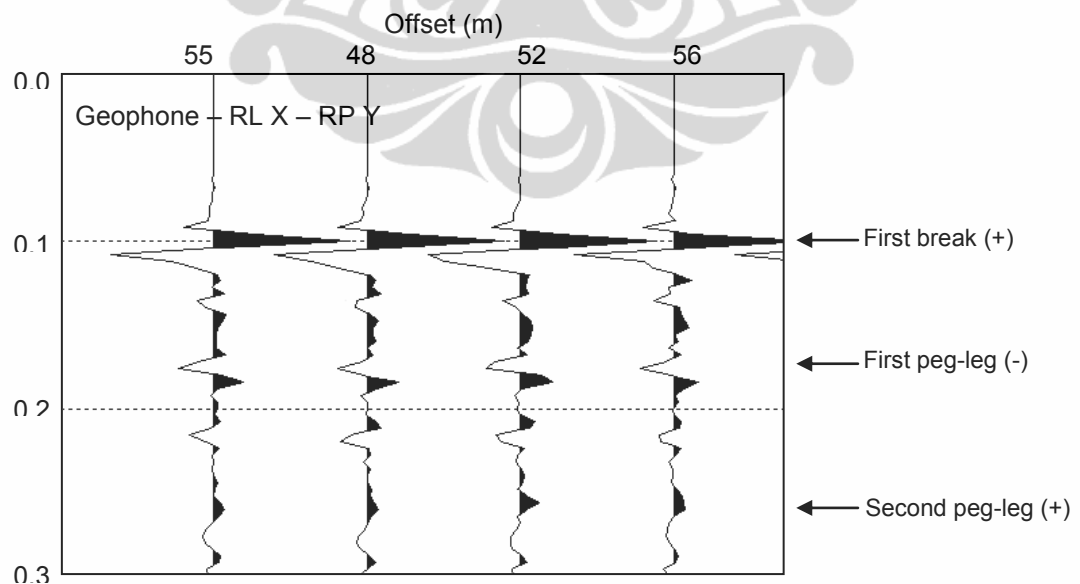


Figure 3.6 Evidence of reverberations on Geophone Data
(60m water depth)

Vice versa with the hydrophone, the maximum of the flattened first break (down-going event) on the geophone data is represented by positive polarity, continued by first peg-leg is negative, and the second reversing again to positive.

Matching operators from geophone to hydrophone, computed on the flattened first breaks (0.060-0.140ms window) per receiver ensembles using offsets limited to 60m.

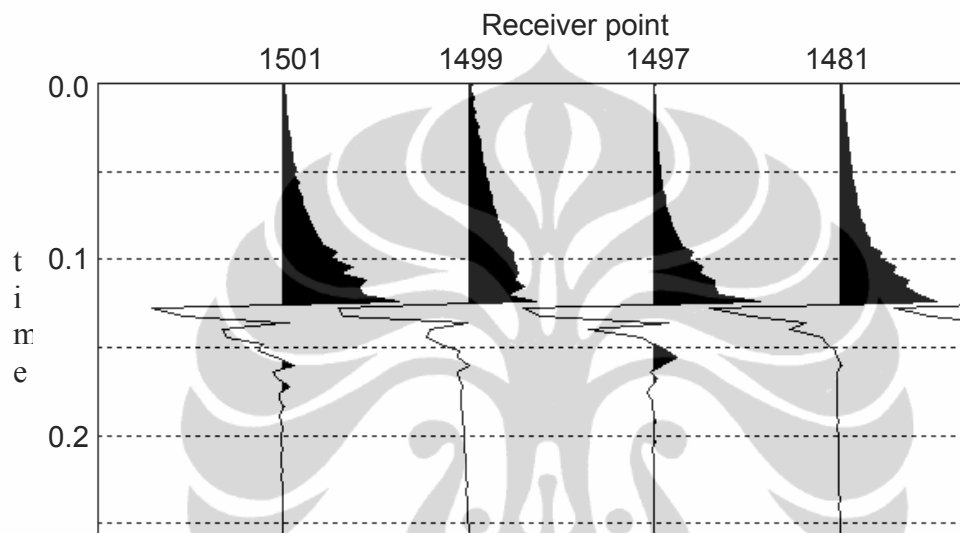


Figure 3.7 Example for Wavelet Operator from several point

This operator were likely uniform from each point, so it can be applied into geophone data, that make geophone data calibrated to hydrophone. On this step, geophone signal is already calibrated but not yet scaled, The Amplitude scaling will be done using hodogram analysis.

3.3 Amplitude Calibration using Hodogram Analysis

After the geophone being calibrated with the wavelet operator that calculated on step above, it is assumed that between geophone and hydrophone is already in same phase when recording a primary event (any upgoing events) and also when recording a ghost or a pegleg (any down going events). Hodograms is plotting between Hydrophone and calibrated geophone amplitude energy. Naturally the primary event will be gathers around the $+/+$ and $-/-$ quadrants, meanwhile down going event will be gathers around the $+/-$ and $-/+$ quadrants. Random noise

should show as “circles” of smaller magnitudes at the center. Destructive interferences between primaries and ghosts or peg-legs should show as “ellipses” between the branches of the cross, with reduced amplitude. It shown in figure below :

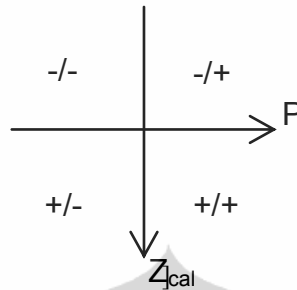


Figure 3.8 Hodograms Concepts

A matching operator was computed from the wavelet of the “S” Horizon at each subsurface bin location. “S” horizon is being chosen, because it provide a favorable working window for amplitude calibration, which this horizon represented of interface from a karstified limestone layer with strong reflection coefficient that appears in whole survey area that will be used to matching scalar process, the hodograms analysis is shown below are example from one bin line and in working window of “S” horizon [-100,200]ms :

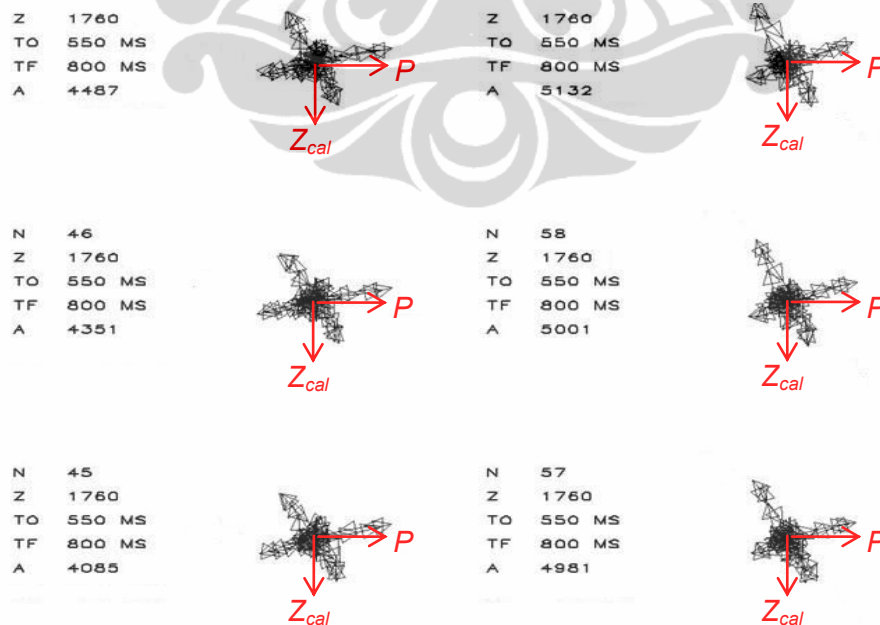


Figure 3.9. Hodograms calculated from [-100,200]ms from S Horizon

Once the hodograms drawn between Z_{cal} (the wavelet-calibrated Z) and $-P$ are built in a window around a strong reflector, including its ghost, the two main directions can be detected, one through the quadrants of same polarity, indicating the primary direction and the second through the other quadrants, indicating the reverberations direction.

If θ is the angle (>0) from Z_{cal} to the direction of the reverberations, toward $-P$, a rotation of the system $(Z_{cal}, -P)$ of angle θ results in the Dual sensor summation as the second rotated vector in the direction orthogonal to the reverberations one (then ghost-free). In other words, $\text{tg}(\theta)$ is the amplitude scalar to scale the wavelet-calibrated geophone before summation.

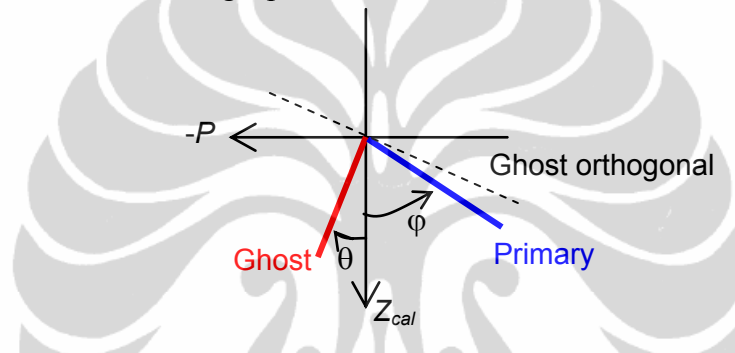
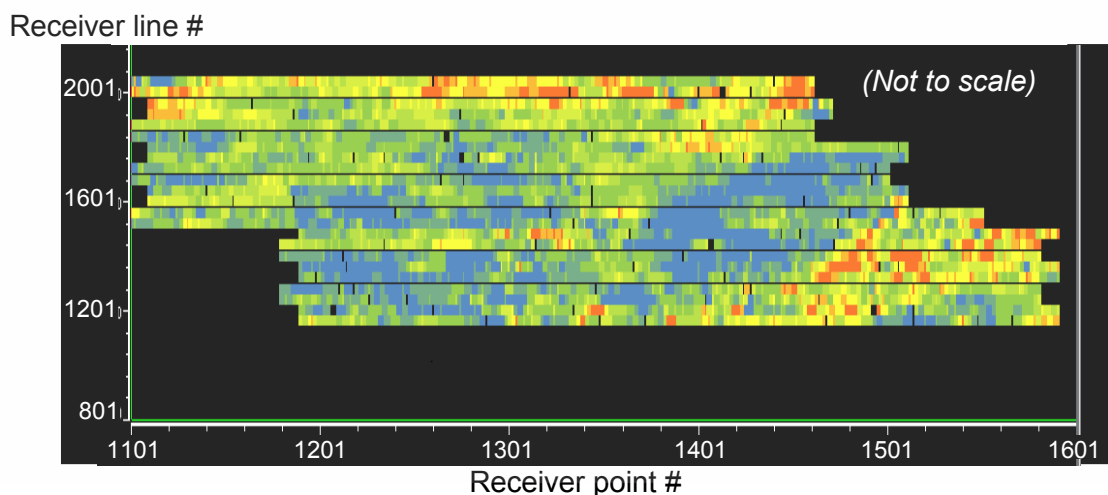


Figure 3.10 Matching Scalar calculation from Hodogram Analysis

The main direction pointing to the primary energy is given by an angle φ , allowing for normalization of the amplitudes of the P and Z_{cal} primaries. The ratio computed on the reverberations after this normalization, given by $\text{tg}(\theta_N)$, provides a way to derive the downward reflection coefficient at the sea floor.

Following is the map of the values found over area from PZ sum built before migration.



Max = -0.3

Min = 0.6

Mean = 0.25

Dominant = 0.32

Number of receiver points: 4553

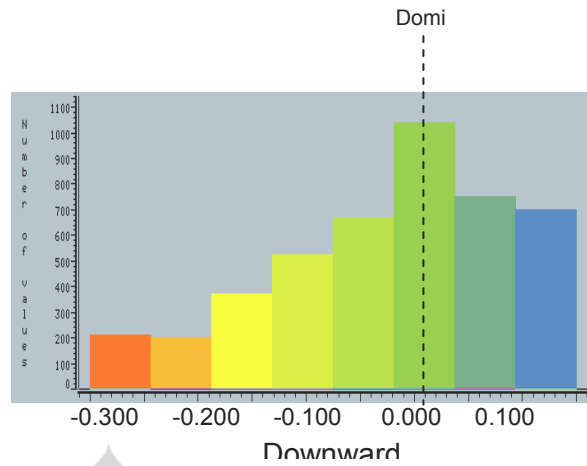


Figure 3.11 Downward Reflection coefficient and it histogram.

In this map, seen that values for amplitude scaling that calculated from hodogram analysis is between -0,3 to 0.6, and being applied on each receiver point attribute, and ready to being sum between P and Z data.

CHAPTER 4

RESULT & DISCUSSION

It has been shown on the previous chapter that Dual Sensor summation works for eliminating ghost effect that appears on data, especially on the main target. But there are pre-conditioning process that should be done to reduce data that not coming from ghost phenomenon, such as reverberation and peg leg is completely attenuated. In the time domain, it clearly seen that ghost effect was appear between top and base reservoir. In hydrophone we seen ghost phenomenon appears as opposite polarity compare to the primary data, and vice versa on the geophone, ghost appears with the same polarity compare to the primary data. and it completely removed after Dual Sensor summation process, shown in figure below :

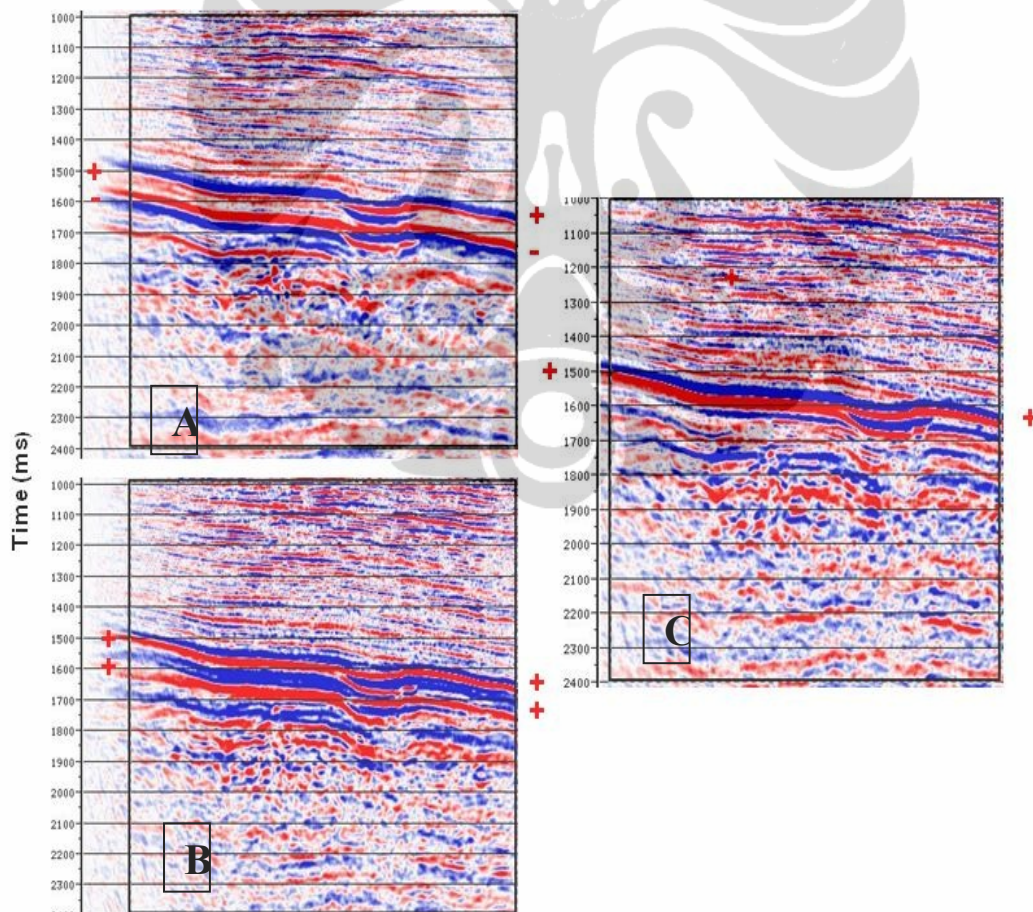


Figure 4.1 Time Domain Comparison (A) Hydrophone Sensor, (B) Geophone Sensor & (C) Dual Sensor

In the frequency domain, it can also be seen clearly that frequency of hydrophone and geophone data are absolutely showing good result after Dual Sensor which is shown with the notch frequency that exist is being summed with Dual Sensor summation resulting for more stabile frequency bandwidth. Several notch that clearly appears on the hydrophone and geophone from water depth 80m. Using equation (2.1) the notch frequency will appears on 18.75 Hz, 37.5 Hz, ...)

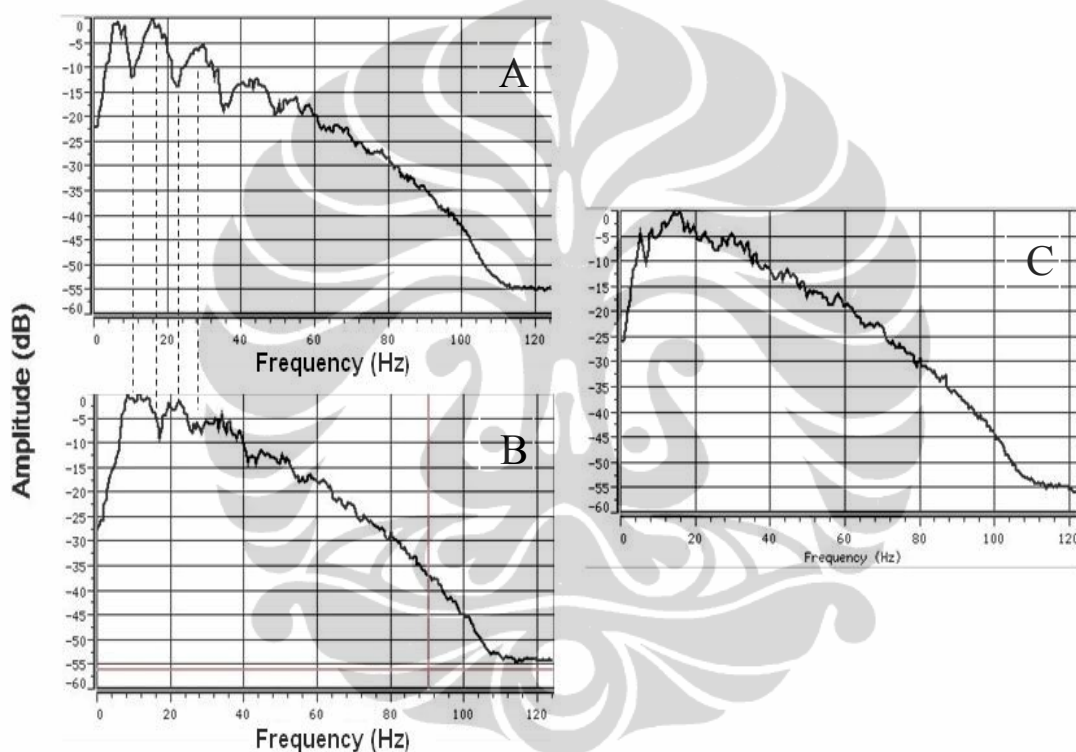


Figure 4.2 Frequency Domain comparison (A) Hydrophone sensor, (B) Geophone Sensor, (C) Dual Sensor

From Frequency and Time domain, it shown us that dual sensor summation process that done in this data set, showing really good improvement on the result, It means the each process, from matching operator analysis and amplitude calibration process suited to assumption that being explained in the theoretical background. Following figure will show a comparison between P data, Z data, PZ data that being done before stacking process and also after stacking process.

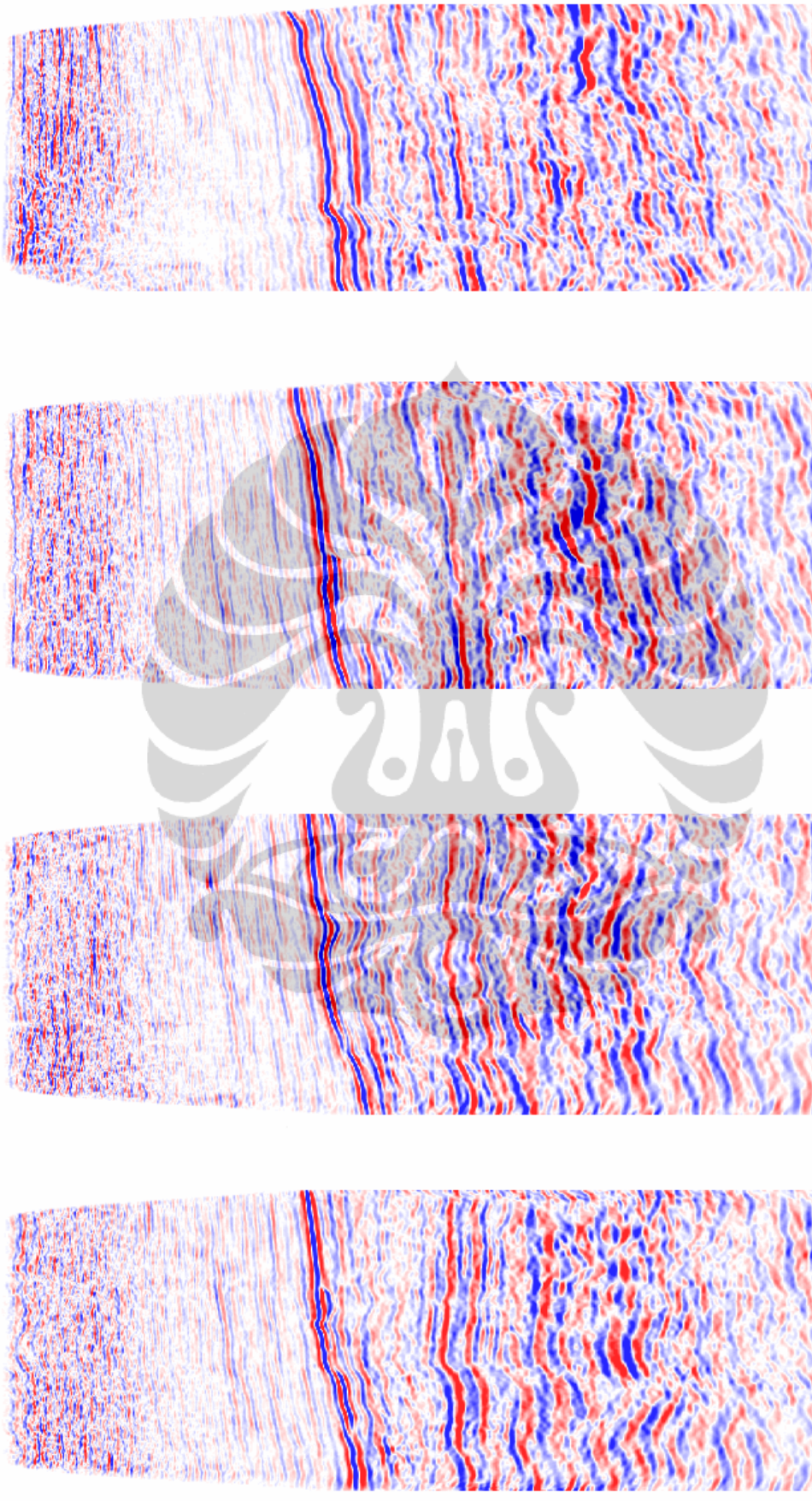


Figure 4.3 Time Migrated PZ Sum Before Stack from several inline (a) Line 1360, (b) Line 1548, (c) Line 1736, and (d) Line 1932.

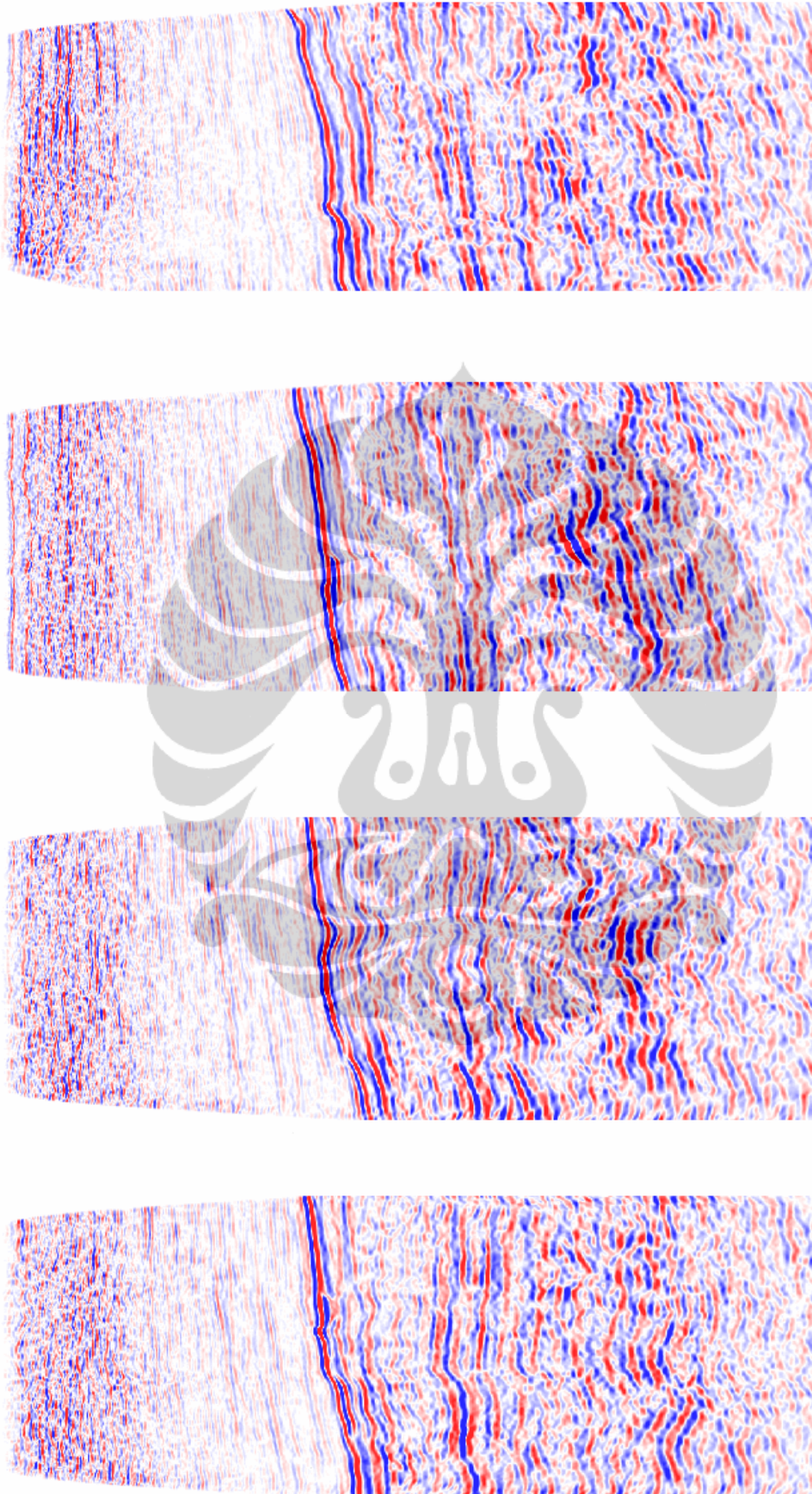


Figure 4.4 Time Migrated PZ Sum After Stack from several inline (a) Line 1736, (b) Line 1548, (c) Line 1360, and (d) Line 1932.

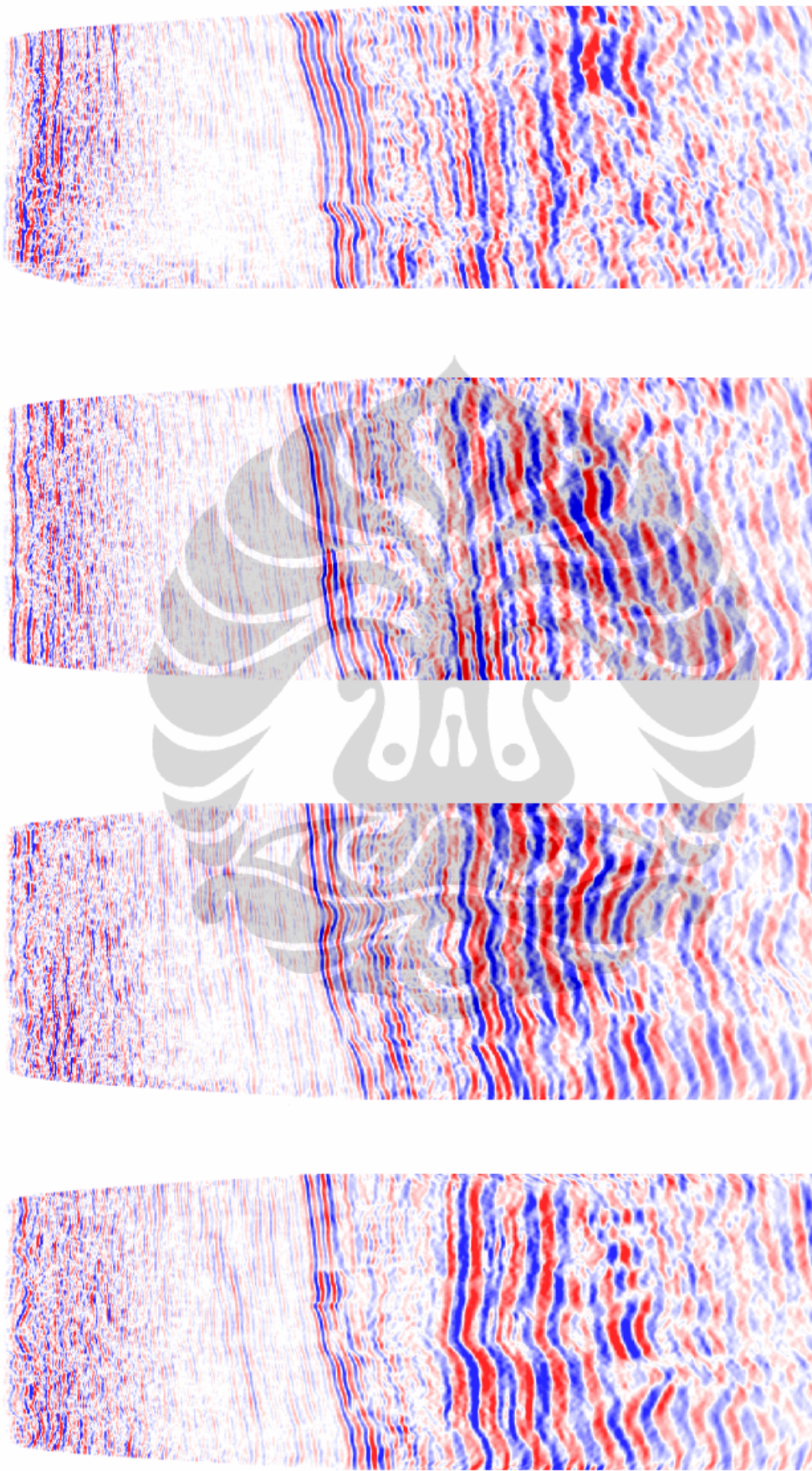


Figure 4.5 Time Migrated P Stack from several inline (a) Line 1360, (b) Line 1548, (c) Line 1736, and (d) Line 1932.

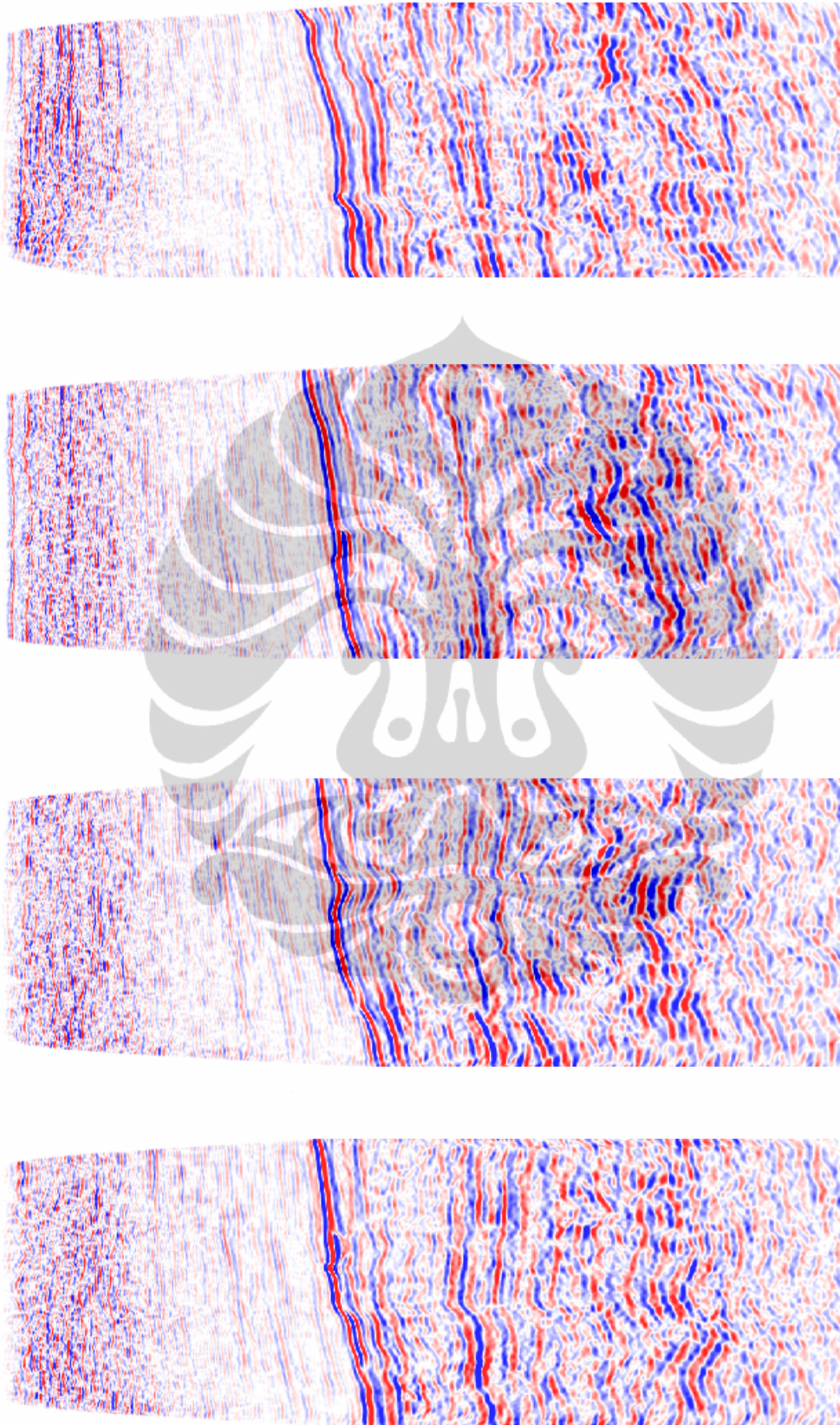


Figure 4.6 Time Migrated Z Stack from several inline (a) Line 1360, (b) Line 1548, (c) Line 1736, and (d) Line 1932.

Whole this PZ process that explained above are done pre stack, or also known considering receiver point attributes, there are also other ways that more simple for PZ summation process, on post stack modes.

A global matching operator between the P and Z stacked datasets was derived in two parallel ways:

1. Computation of the matching operator at each subsurface bin location between the wavelets taken on the strong "S" horizon. The global operator was built by averaging the operators computed at each bin location.
2. Reduction of the matching operator to a phase rotation (50deg was finally selected) between the two images.

The Z image was then calibrated using successively the two global operators and a residual amplitude calibration factor was computed at each bin location, from the hodogram built with the hydrophone trace and the calibrated geophone one, considered the two components of a vector.

Hodograms with different matching operators (PZ after stack)
Matching operator= 80deg phase rotation (hodogram in 250ms window around "S", including its ghost, bin line 1760):

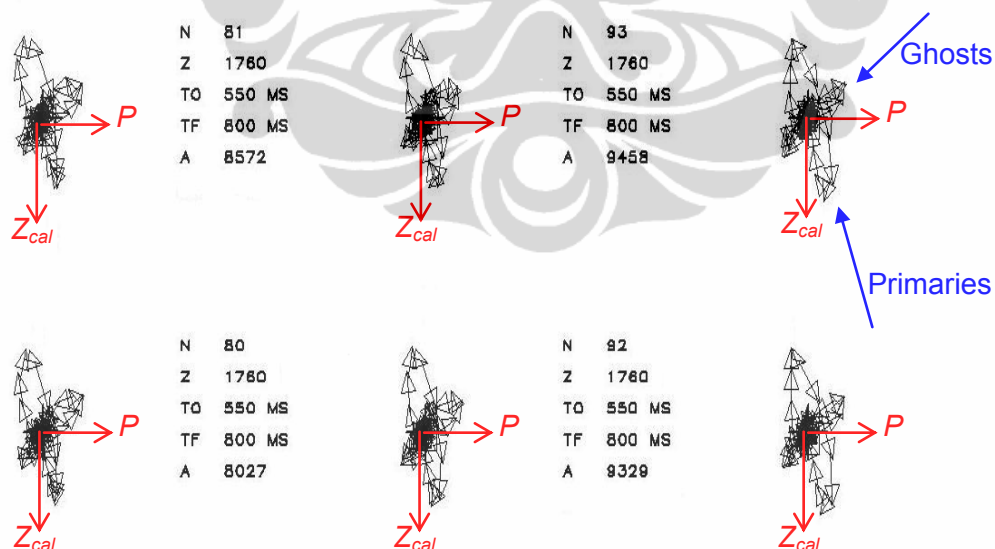


Figure 4.7 Hodogram with phase rotation 80 deg, [250]ms window

Matching operator= 50deg phase rotation (hodogram in 250ms window around "S", including its ghost, bin line 1760):

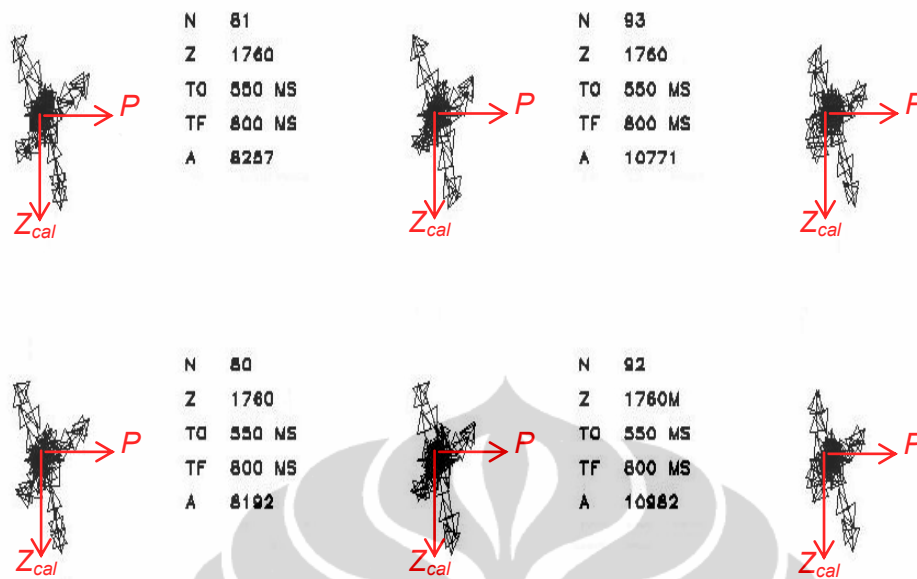


Figure 4.8 Hodogram with phase rotation 50 deg, [250]ms window

The second operator allowed for better polarized events and was preferred to the first one, although the directions of the branches of the cross look fairly identical.

The validity of the operation was controlled:

1. In time domain, by comparison of the sum with images built from streamer data in the same area, (receiver ghost-free, at least around the 25-30 Hz dominant frequency), on the “S” horizon
2. In frequency domain: by cancellation of the notches.

Figure shown below will shows the validity operation that being explained above :
 Example: Line 1660: After time-migration (no post-stack processing)

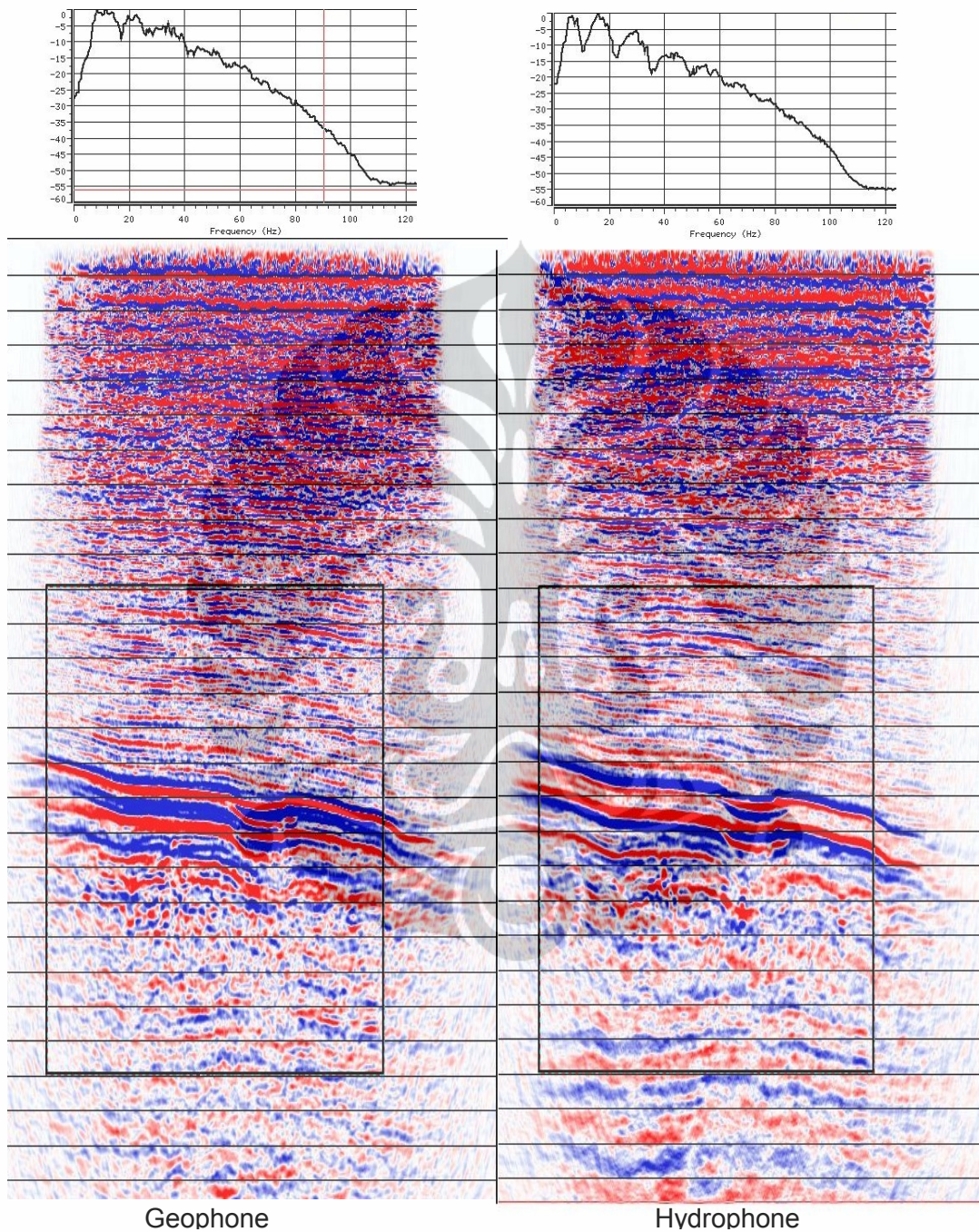


Figure 4.9 Geophone Stack that already phase shifted 50 deg and amplitude calibration from hodogram (Left) and Hydrophone Stack (Right) with frequency contents on target area.

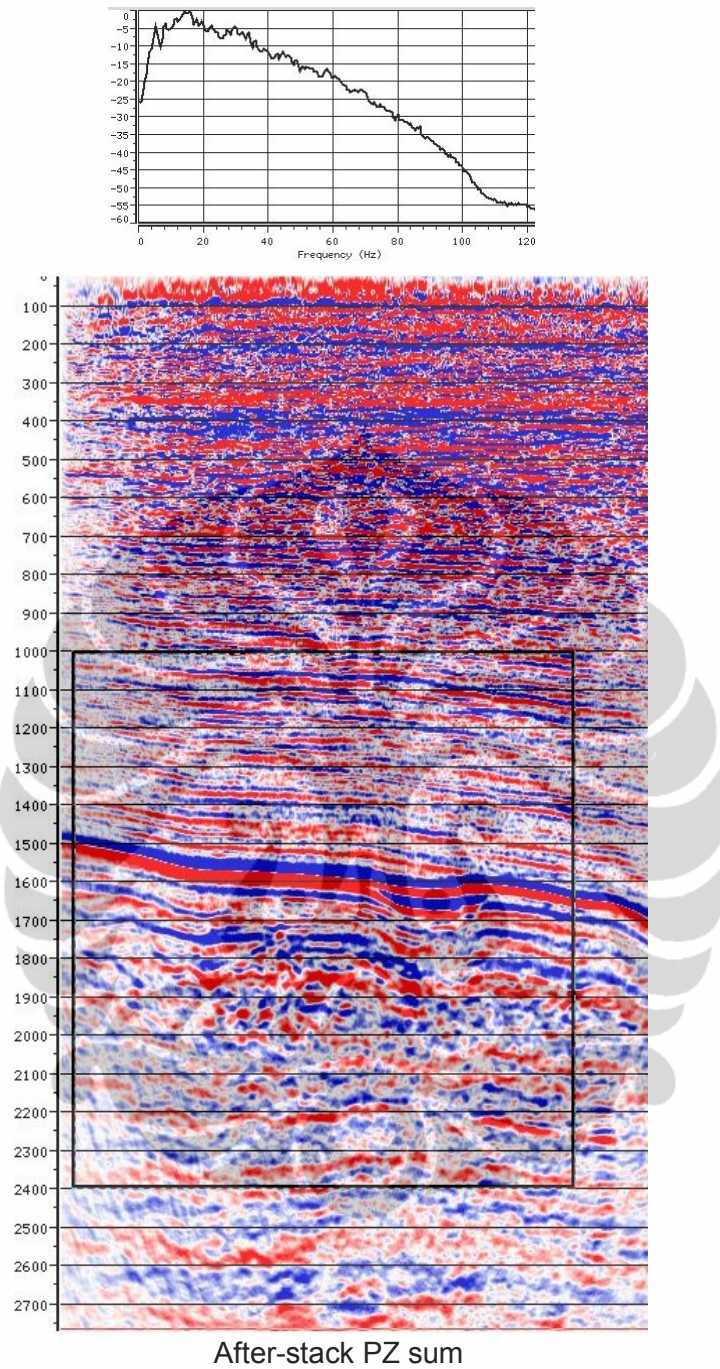


Figure 4.10 PZ Summation done after Stack and frequency contents.

CHAPTER 5 CONCLUSION

PZ sum requires the wavelet differences between the P and Z responses to be prior removed. These differences are mostly receiver attributes attached to the receiver point and the natural domain of addressing them is receiver mode. Calibrations need all the components of the signal, including primary and the reverberation train to be recognized and dominant among the noise.

Strong noise is a common element in OBC data. Recent development considered its removal the main point of the summation and it was decided to follow this trend and independently process the P and Z data sets as far as after stack where noise is considered insignificant. The reverberations train was first processed by a gapped tau-p deconvolution but a remaining strong ghost could not be attenuated without summation, as clearly shown on the spectra of the final P and Z stacks. Calibration was first done post-stack ignoring the receiver attribute type of the ghost effect and it is believed that this would work as long as the frequency notches are in accordance with the theory.

PZ sum was repeated before migration. The receiver attribute type formulation could be recovered but the reverberations train, already processed by deconvolution, could not be considered intact. Although not at the same optimum level of denoising as for the first method, calibration was done after several passes of noise attenuation.

Both approachment benefited from the signal to noise ratio improvements that are not given by an early calibration. Some differences remain in the images produced by the two summations.

Dual sensor recording is the obvious solution to ghost removal but that there is no general calibration process, which has to be adapted to all kinds of environments (shallow water, presence of identified and strong markers, etc) The processing geophysicist must always be very cautious in the two calibration steps (matching operator derivation and amplitude factor) and take decisions according to the particular datasets.

Matching operator can be computed when a wavelet can be extracted for both sensors (that means enough water depth and PO lines). If the operator can be selected short (good coupling), cross-ghosting can be used in a convenient window on reflections.

For amplitude calibration, hodographs can be used if a strong marker is dominant with its ghost. otherwise, scan and tests must be done with the appreciation of the interpreter.



REFERENCES

- Ball, Vaughn., and Corrigan, Dennis., 2004, Dual-sensor summation of noisy ocean-bottom data .SEG Expanded Abstract.
- Barr, Fred J. and Sanders, Joe I., 1989a. Attenuation of water-column reverberations using pressure and velocity detectors in a water-bottom cable: Expanded Abstracts of the 59th Annual SEG Meeting, TX, p. 653-656.
- Barr, Fred J., 1997. Dual Sensor OBC Technology:The Leading Edge January 1997.
- Shoshitaishvilli, Elena. and Mitchell, Scott.,2006, Imaging Subsalt target using OBS data in deepwater Gulf of Mexico: 2D synthetic data example. SEG New Orleans Annual Meeting.
- Soubaras, R., 1996, Ocean-bottom hydrophone and geophone processing: 66th Annual International SEG Meeting., Expanded Abstracts, 24-27.
- Specht, J., 2007, Differential OBC Processing Techniques : SEG Antonio Annual Meeting.
- Ugbor, C.C.,2007, First Dual-Sensor Ocean Bottom Cable 3D Seismic Acquisition South Atlantic Ocean , offshore Niger Delta, Nigeria. Pacific Journal of Science and Technology.8(1):36-48.